

THESIS FOR THE DEGREE OF LICENTIATE OF
ENGINEERING

**Parameter Estimation of a DOC from Engine
Rig Experiments**

BJÖRN LUNDBERG



Chemical Engineering
Department of Chemical and Biological Engineering
CHALMERS UNIVERSITY OF TECHNOLOGY
Göteborg, Sweden 2013

Parameter Estimation of a DOC from Engine Rig Experiments
BJÖRN LUNDBERG

© BJÖRN LUNDBERG, 2013

Licentiatuppsatser vid Institutionen för kemi- och bioteknik, Chalmers tekniska högskola
Serie nr 2013:14
ISSN 1652:943X

Chemical engineering
Department of Chemical and Biological Engineering
Chalmers University of Technology
SE-412 96 Göteborg
Sweden
Telephone: +46(0)31-7721000

Chalmers Reproservice
Göteborg, Sweden 2013

PARAMETER ESTIMATION OF A DOC FROM ENGINE RIG EXPERIMENTS

Björn Lundberg
Department of Chemical and Biological Engineering
Chalmers University of Technology
SE-412 96 Göteborg, Sweden

ABSTRACT

In this thesis methods of parameter estimation of a Diesel Oxidation Catalyst (DOC) from engine rig experiments were investigated. The investigation did not only include methods of parameter fitting to experimental data but a large effort was also put into catalyst modeling and experimental design.

Several different catalyst configurations were used with varying Pt loading, washcoat thickness and volume. To further expand the experimental space, engine operating points were chosen with a wide variation in variables (inlet conditions) and both transient and stationary operation was used. A catalyst model was developed where the catalyst washcoat was discretized as tanks in series both radially and axially and for parameter estimation a traditional gradient search method was used. Four different modeling approaches were used for parameter tuning where the most successful one tuned kinetic parameters as well as internal mass transfer parameters. It was also shown that it is of high importance that the kinetic model used has an intrinsic structure when the catalyst model separates mass transport and kinetics and when several catalyst configurations are used.

A new method was evaluated where sensitivity analysis and data selection was used as a part of the parameter estimation. The data selection was made by D-optimal design of an approximation of the sensitivity matrix using Principal Component Analysis. This methodology renders better statistical properties and should improve the parameter tuning when using gradient search methods. Furthermore, a reduced computational cost could be achieved

by using only the most relevant data points during parameter tuning. To make a relevant comparison possible the same catalyst model and experimental data was used as in the previous evaluation of modeling approaches. However, the evaluated method did neither result in an improved fit to measurement data nor reduce the time for parameter tuning compared to the reference case. Adjustment of an unbalanced weighting of the residuals for the different components NO, hydrocarbons, CO, and NO₂ was identified as the most important factor for a future improvement of the method. More transients in the measurement data and updated parameter weighting were other suggested measures to improve the method.

When performing catalyst modeling and parameter tuning it is desirable that the experimental data contain both transient and stationary points and can be generated over a short period of time. A method of creating such transients in concentration for a full scale engine rig system was presented and evaluated. The method included an engine rig where an SCR with urea injection and a DOC with bypass possibility was used as part of the experimental setup. The DOC and SCR with urea injection were positioned between the test object, which also was a DOC, and the engine. By controlling urea injection and DOC bypass a wide range of exhaust compositions, not possible by only controlling the engine, could be achieved which will improve the possibilities for parameter estimation for the modeling of the DOC in future studies.

Keywords: Exhaust Aftertreatment Modeling, DOC, Full Scale, Design of Experiments, Parameter Estimation, Engine Test Bench, Multivariate Data Analysis

ACKNOWLEDGEMENTS

I would like to take this opportunity to express my gratitude to all of those who helped me finish writing this thesis.

First I would like to thank all of my supervisors and Professor Bengt Andersson for giving me the opportunity to do my PhD at Chalmers in this interesting field of research. I would like to thank my supervisors at Chalmers, Professor Derek Creaser and Assistant Professor Jonas Sjöblom, for always encouraging me and for many rewarding discussions. Every time I've thought I've reached a dead end you have helped me find a new path to explore, your guidance has been invaluable. I would also like to thank my industrial partners Johnson Matthey and Scania AB, and in specific my industrial supervisors Dr. Åsa Johansson and Dr. Björn Westerberg. Thanks for valuable input and discussions during our monthly meetings and for making me feel welcome during my visits in Högsbo and Södertälje.

I would like to thank all present and former colleagues at the Chemical Engineering Department for a relaxed atmosphere and for enjoyable discussions, both work related and not. Sometimes I feel very lucky to have colleagues who drop by my office (if you're not already in it for some reason) and make me forget about my work from time to time, I could thank you all by names but you all know who you are. I would also like send my gratitude to Ingrid for convincing me to apply for this position; I have not regretted it for one second.

Financial support from Swedish Energy Agency and from ÅForsk is gratefully acknowledged. Also thanks to Swedish National Infrastructure for Computing (SNIC) at C3SE for the computational resources used in this project.

Finally but not least I would like to thank my friends and family for being there and supporting me and for reminding me that there are more important things in life than work.

LIST OF PUBLICATIONS

This thesis is based on the following enclosed papers where I was responsible for writing, planning and supervising experiments, data analysis, and computation:

- I** **Parameter Estimation of a DOC from Engine Rig Experiments with a Discretized Catalyst Washcoat Model**
Björn Lundberg, Jonas Sjöblom, Åsa Johansson, Björn Westerberg and Derek Creaser
Submitted
- II** **Parameter Estimation of a DOC by Model-based Experimental Data Screening from Engine Rig Experiments**
Björn Lundberg, Jonas Sjöblom, Åsa Johansson, Björn Westerberg and Derek Creaser
Manuscript
- III** **New Methodology for Transient Engine Rig Experiments for Efficient Parameter Estimation**
Björn Lundberg, Jonas Sjöblom, Åsa Johansson, Björn Westerberg and Derek Creaser
Submitted

The following papers have not been included in the thesis:

- IV** **Characterization of Particulate Matter from Direct Injected Gasoline Engines**
Carolin Wang-Hansen, Per Ericsson, Björn Lundberg, Magnus Skoglundh, Per-Anders Carlsson and Bengt Andersson
Submitted to *Topics in Catalysis*
- V** **Modeling Study of 5 kWe-scale Autothermal Diesel Fuel Reformer**
Derek Creaser, Karatzas Xanthias, Björn Lundberg, Lars Pettersson and Jazaer Dawody
Applied Catalysis A: General, 2011. 404(1-2): p. 129-140.

TABLE OF CONTENTS

1	INTRODUCTION	1
1.1	Heavy Duty Diesel Engines Environmental Issues	1
1.2	Heterogeneous Catalysis	2
1.3	The Role of the DOC in the Aftertreatment System	3
1.4	Objectives	4
1.5	Method Overview	6
2	DESIGN OF EXPERIMENTS	9
2.1	Principal Component Analysis	11
2.2	D-optimal Design	12
3	EXPERIMENTAL	15
3.1	Catalyst Configurations	15
3.2	Engine Rig Experiments	16
3.2.1	Set-up	16
3.2.2	Experimental design	18
3.3	Scania Engine Rig	20
3.3.1	Set-up	20
3.3.2	Experimental design	21
4	MODELING	23
4.1	Reactor model	23
4.1.1	Mass transport	26
4.1.2	Heat Transport	28
4.1.3	Discretization	29
4.2	Kinetic Model	31
5	PARAMETER ESTIMATION	35
5.1	Adjustable Parameters	35
5.1.1	Kinetic Parameters	36
5.1.2	Heat Transport Parameters	37
5.1.3	Mass Transport Parameters	38
5.2	Standard Method of Parameter Estimation	39
5.2.1	Gradient search method	39
5.2.2	Residual weighting	41

5.3	Parameter Estimation aided by PCA and D-optimal Design	42
5.3.1	Method	42
5.4	Computational Efficiency	46
5.4.1	Paralellization	46
5.4.2	Cluster Computation	48
6	RESULTS AND DISCUSSION	49
6.1	Paper I – Traditional Parameter Estimaion on a Full Scale DOC	49
6.1.1	Modes of Parameter Estimation	49
6.1.2	Heat Transfer Parameter Tuning	50
6.1.3	Tuning of Kinetic- and Mass Transfer Parameters	51
6.2	Paper II – Parameter Estimation with MVDA on a Full Scale DOC	53
6.2.1	MVDA Approaches	54
6.2.2	Fit to Measurement Data Comparison	54
6.2.3	Computational Efficiency Comparison	56
6.2.4	Conclusions	58
6.3	Paper III – New Methodology for Transient Engine Rig Experiments	58
7	CONCLUSIONS	63
8	OUTLOOK	65
	BIBLIOGRAPHY	67

1 INTRODUCTION

1.1 HEAVY DUTY DIESEL ENGINES ENVIRONMENTAL ISSUES

The complete combustion of fossil fuel and air results in emission of CO₂ and H₂O. However the combustion in heavy duty diesel (HDD) engines, and other internal combustion engines, will never be complete which leads to the formation of CO, un-burnt hydrocarbons (HC), and also particulate matter such as soot in addition to CO₂ and H₂O [1]. The high temperatures in the engine during combustion will also lead to the formation of nitrogen oxide (NO_x) from oxygen and nitrogen in the intake air [2].

CO, CO₂, HC, NO_x, and particulate matter are all major contributors to air pollution and in today's cars and trucks all of them except CO₂ are reduced in the after treatment system. The environmental issues associated with diesel engine exhaust are both numerous and diverse. CO poisoning is the most common type of fatal air poisoning worldwide [3] as it, even in small concentration, can severely hinder the delivery of oxygen to organs and tissues [4]. NO_x contributes to the acidification of land and lakes [5], has toxic effects on the respiratory system and can also in combination with HC produce ground level ozone [3]. Some of the different hydrocarbons produced by combustion are also considered carcinogenic to humans [6]. Exposure to urban particulate matter can lead to increased risk of a variety of respiratory diseases and adverse health effects such as lung cancer, bronchitis and asthma [7].

The current European emission standard for HDD, which regulates emissions of CO, HC, NO_x, and particulate matter, is called Euro V and was introduced in 2008. In December 2013 the Euro VI will be introduced which

will even further reduce the limits for HC, NO_x, and particulate matter emissions. To meet these and forthcoming legislations an increased understanding of the after treatment system will be of utmost importance.

1.2 HETEROGENEOUS CATALYSIS

The common structure of a catalyst in the automotive industry is a monolith of flow through type with a shape that is generally cylindrical with quadratic channels. The catalyst can be divided into two parts; the porous washcoat that carries the active material where the reaction takes place (B in figure 1) and the solid substrate that gives the catalyst its' structure (A in figure 1). The substrate in the current study is made of cordierite that is a ceramic material with low density (ca 400 kg/m³), high heat conduction and stable thermal properties. To get an efficient mass and heat transfer between the gas phase (exhaust gas) and solid phase (the washcoat) a large interfacial area is favorable. This is achieved by making the number of channels per catalyst cross sectional area very large and as an example all catalyst configurations used in the current study have 62 channels per cm².

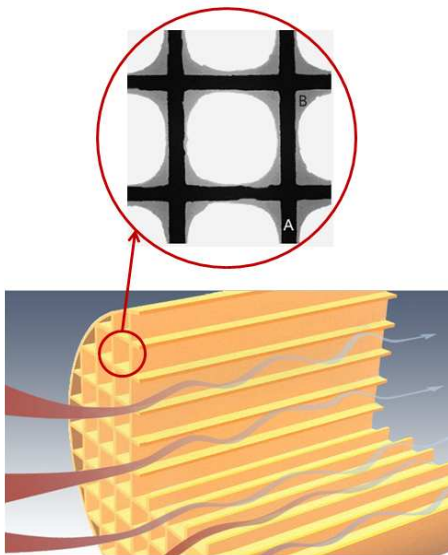


FIGURE 1 *Monolith and washcoat*

The washcoat is coated on the inside of the walls of the substrate and forms a thin porous layer through which the exhaust needs to diffuse to react with the active material. Again to get a high interfacial area between the exhaust

gas diffusing through the washcoat and the active material a large washcoat area per washcoat volume is desirable. High surface area materials such as γ -alumina are therefore commonly used as the primary washcoat material. Several types of active materials are possible but for automotive oxidation catalyst noble metals, such as platinum and palladium, are most common.

1.3 THE ROLE OF THE DOC IN THE AFTERTREATMENT SYSTEM

The diesel oxidation catalyst (DOC) is a well established technology to reduce CO and hydrocarbon (HC) emissions from diesel engines that has been in use since the 1970s. Strengthened emission standards have made the importance of the DOC even greater in recent years since it has become an indispensable component for enhancing the performance of diesel particulate filters (DPF) and selective catalytic reduction (SCR) catalyst by utilization of oxidation of NO to NO₂.

Three reactions are desirable in the DOC; the oxidation of CO to CO₂, the oxidation of HC to CO₂ and H₂O, and the oxidation of NO to NO₂. In other words, the DOC does not remove any NO_x but adjusts the NO₂/NO_x ratio which is important later in the aftertreatment system.

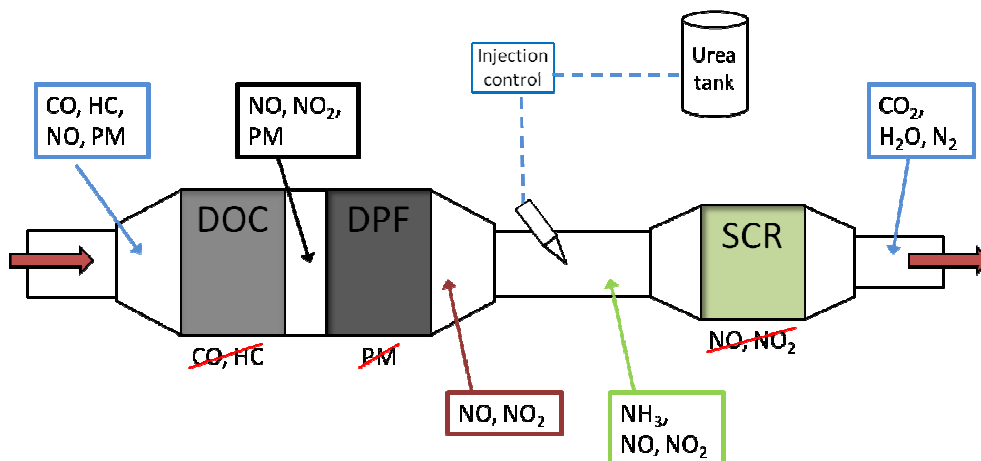


FIGURE 2 Typical layout of an aftertreatment system used for heavy duty diesel vehicles [8]

Figure 2 shows a typical layout of an aftertreatment system used for heavy duty diesel vehicles based on urea-SCR for controlling NO_x emissions. At ideal conditions both HC and CO has been fully oxidized in the DOC and the only

pollutants left are NO_x and particulate matter (PM). The PM is trapped by the DPF and depending on if an active or passive regeneration (PM oxidation) strategy is employed the performance of the DOC will be of different importance. If passive DPF regeneration is used the DOC will be needed to provide NO_2 that enables PM oxidation at lower temperatures [9]. If active DPF regeneration is used, on the other hand, the temperature will be periodically increased so that PM can be reduced by O_2 , [9] in this case the DOC performance is of less importance. However, even for an active DPF regeneration strategy a simultaneous passive regeneration is also usually desirable which means that the DOC performance still will be of some importance. In fuel efficiency perspective the passive DPF is preferable since extra fuel injection is needed to perform the active DPF regeneration.

In the SCR, NO_x will be reduced to N_2 with NH_3 from the decomposition of injected urea. The desirable reaction here is the so called fast SCR reaction where equal amounts of NO and NO_2 are consumed [10]. The reactions in the SCR will therefore be dependent on the NO_2/NO_x fraction out from the DOC. To conclude the DOC will be crucial for the performance of the SCR and, depending on what DPF regeneration method is used, may also be of great importance for regeneration of the DPF.

1.4 OBJECTIVES

To estimate kinetic parameters, laboratory scale experimental data is generally used [11]. In laboratory scale it is possible to use essentially any combination of exhaust gas composition and temperature which makes it possible to estimate parameters over a wide range of conditions. However the validity of these parameters in full scale models is often limited and therefore the parameters commonly need to be retuned. It is this retuning of parameter values from lab scale to full scale that is the objective of the current work and the reason why experiments are performed in an engine rig. The tuning of kinetic parameters are also complemented by tuning of heat and mass transport parameters to better describe the dynamic behavior of the full scale catalyst. It should be noted that the concept of *parameter estimation* is better known and will be used throughout the current work even though parameter retuning may be a more accurate description.

Efficient parameter estimation has several aspects. The design of experiments should be carried out in a manner in which the total experimental time is low (since engine rig experiments are very costly to perform) but at the same time the generated experimental data should be information rich and make it possible to estimate parameters sufficiently accurate. This does not only include how the engine is run but also what catalyst configurations are used and the general set-up of the engine rig.

To perform parameter estimation a catalyst model is of course of high importance. Since both kinetic and mass transfer parameters will be estimated it is important to have a model where these phenomena can be separated. The model used needs to be detailed enough to describe the reactions and transport phenomena in a full scale catalyst but it should in the same time be robust and simple to avoid too long simulation times. To find a good trade-off between model accuracy and computational time is therefore an important part of the objective. The parameter estimation itself should also be performed in an efficient way meaning that the time spent at parameter estimation should be reduced. In section 1.5 Multivariate Data Analysis (MVDA) is introduced as a way of both reducing the number of data points used for simulation and to more efficiently reach the goal of approaching the global minima. An important part of making the parameter estimation more efficient is also to optimize the use of computational resources. This could for example mean running simulations in parallel on multiple processor cores either locally or on a cluster to reduce simulation time. It should however not be forgotten that the most important objective is a good fit to measurement data which should not be compromised in the aim of making the parameter estimation time efficient.

To conclude and summarize: the objective is to efficiently estimate kinetic, mass and heat transfer parameters for full scale catalysts from engine rig data. This includes experimental design, catalyst modeling and the method of parameter estimation. The procedure should be fast and robust and also adaptable to different catalyst properties.

1.5 METHOD OVERVIEW

The method applied in the current work can be summed up in four points

1. Design of Experiments (DoE)
2. Engine rig experiments
3. Multivariate data analysis (MVDA)
4. Parameter estimation

Point 1, 2 and 4 were applied in the first parameter estimation performed in Paper I and was extended with MVDA (point 3) in Paper II. Paper I can, in a sense, be viewed as a reference to how parameter estimation is normally performed and Paper II is an attempt to improve it. The full method therefore includes all four points even though they have not been applied in all of the parameter estimation performed in the current work. In Paper III only point 1 and 2 is performed and point 3 and 4 will be applied on the resulting data in an upcoming study. All of the points will be discussed in detail in upcoming sections and this section will only give a brief introduction.

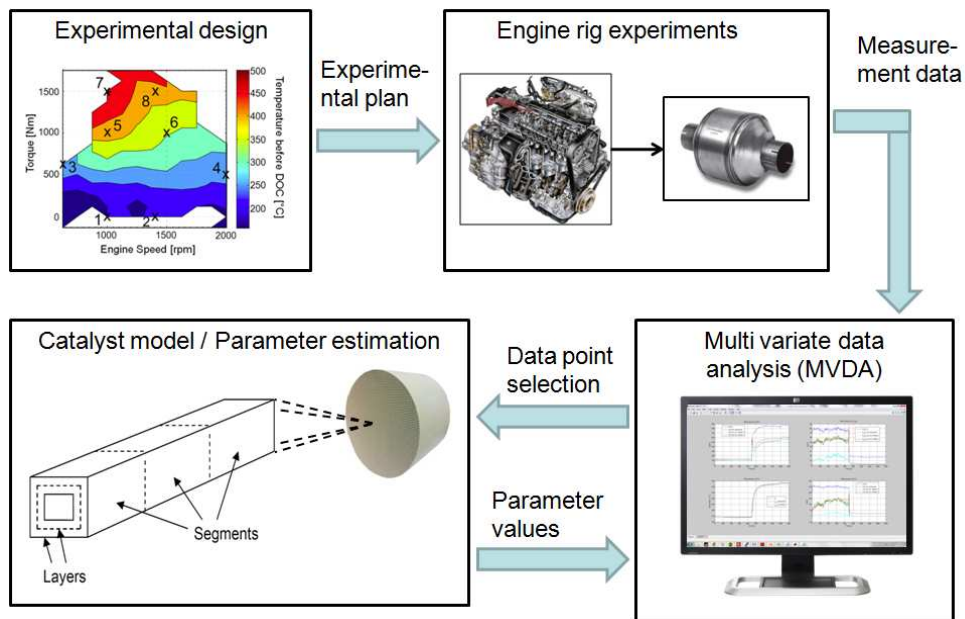


FIGURE 3 *Method overview*

The available variables (exhaust composition, flow, and temperature) of a full scale engine rig are severely limited by the operating points of the engine which is only decided by the engine torque and load. The values of the different variables at different operating points can be described by an engine

map which also indicates what torque and load combinations that are possible. To make sure that the variables are varied as much and as independently as possible an analysis of the map can be performed. From this analysis a set of suitable operating points can be selected with Design of Experiments. It is also possible to vary the catalyst inlet condition with some additional equipment situated between the engine and the catalyst, as demonstrated in Paper III. To further increase the experimental space a number of different catalyst configurations can also be used.

In point 2 the designed experiments are performed in an engine rig where the exhaust composition, flow, and temperature are measured before and after the catalyst. Point 3 and point 4 are strongly connected and the process after the experiments have been performed will here be described as a whole. In the traditional way of performing parameter estimation a gradient search method is used to minimize the residual sum square of all variables in all experimental data points. The method generally gives good results since all experimental data is used but there are some drawbacks such as, long simulation time, risk of finding a local minima far from the global minima, risk of being dominated by certain parameters, and high parameter correlations. In the method using MVDA only the data points with the highest parameter sensitivities are selected for parameter estimation with the gradient search method. This aims to decrease the simulation time and may also reduce some of the other drawbacks with the traditional way of performing parameter estimation.

2 DESIGN OF EXPERIMENTS

Experimental design is a tool used to systematically examine the behavior and properties of a certain system that in the current case is a full scale catalyst of DOC type. If the experiments are performed without structure the results will as well be unstructured and the analysis and eventual parameter estimation will be further complicated. Therefore a good experimental plan is the foundation of successful parameter estimation and should be thoroughly evaluated before any experiments are performed [12, 13].

A first important step in the experimental plan is to identify what variables that can be investigated, what can be measured, and what the interesting responses are. For a full scale catalyst in an engine rig system the composition, temperature and the flow rate both at the inlet and outlet is measured. The inlet conditions are changed by controlling equipment upstream of the catalyst such as the engine itself or even other catalysts. Since the catalyst itself, which is to be modeled, has no influence on the inlet conditions all properties of the flow entering the catalyst must be variables. The outlet conditions on the other hand are a result of the catalyst performance and the response of the system is therefore the measured composition and temperature at the catalyst outlet. If the experiments would have been performed in lab scale on a catalyst in powder form these variables and responses may have been enough, however, in the case where significant mass transport resistance in the washcoat can be expected some variables should also be found that influence mass transport. The variables selected for this purpose in the current study are different catalyst configurations that will have different mass transfer properties.

In the simplest case all the variables can be varied independently and the model is linear and time independent. For a system as complex as a full scale catalyst none of these properties are applicable. The variables that are controlled by the engine operating point are highly correlated and a change in operating point will more or less affect all concentrations, flow rate, and temperature. A method of reducing these correlations is, however, presented in Paper III. The catalyst is also a highly non-linear system which is easy to conclude by only investigating some of the simplest kinetic models describing the DOC and becomes even more obvious when considering that mass and heat transport resistances may also influence its operation.

The large thermal mass of the catalyst also means that energy will be accumulated and thus the properties of the system will not only depend on the current inlet conditions but also on the inlet at earlier time points that may be several minutes earlier if the temperature change is large. The temperature is however not the only variable with a dynamic behavior (just the most dominant one) since also components can be accumulated in the washcoat as surface adsorbed species.

The dynamic behavior of the system means that transient experiments are of utmost importance [14] and should be the central point of any experimental plan for a full scale catalyst system. This is especially true since the system has unobservable variables such as quantities of surface adsorbed species. Different types of transient experiments have been used in the current work where the most frequently used one (Paper I and II) is a simple step change in the engine operating point. A simple transient like that does however significantly increase the parameter space and improves the conditions for parameter estimation [15].

When input variables can be varied independently (applied to a linear model) it is possible to make an orthogonal design. In a system where the variables are inherently correlated the Design of Experiments should strive to make the design of experiments as orthogonal as possible. Also the parameters that are to be estimated may be correlated, this is however an issue that will be further discussed in sections 2.1 and 2.2.

2.1 PRINCIPAL COMPONENT ANALYSIS

Principal Component Analysis (PCA) is a mathematical method where large sets of observations of possibly correlated variables are transformed into new, linearly uncorrelated variables. The number of uncorrelated variables, usually referred to as principal components, is usually chosen to be fewer than the number of variables in the untreated data [16].

The PCA can be performed with several different purposes such as identification of classes of data and outliers, simplification, data reduction, modeling, variable selection, and prediction. A simple way of describing the method would be as an approximation of a data matrix where the more similarity within the objects result in fewer terms needed for a good fit.

In the first step of transforming a set of data (X) according to PCA the direction that captures the largest variation in the data is identified via least squares. The normalized vector describing the identified direction will be the first principal component in the transformed set of data (see figure 4). Another principal component can be added by again identifying the direction that captures the largest variation in the data but now with the added criterion that the direction must be orthogonal to the first principal component (see figure 4). Components are usually added to the PCA-model until the increase in information with the added component is below a certain limit. The matrix containing the principal component vectors is called the loadings vector and can be used to analyze the relation between variables.

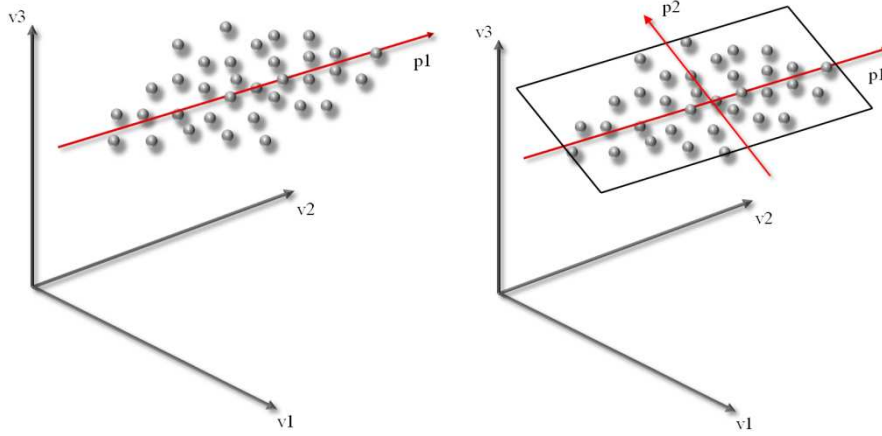


FIGURE 4 *First (left) and second (right) principal components of an arbitrary data set with three variables.*

The observations (rows) are projected onto the sub-space defined by the principle components which will result in a number of vectors (as many as the number of principle components) that are orthogonal but not normalized. The vectors are summarized in the scores matrix that can be used to analyze the relations between observations.

In the current study PCA was used in Paper II to select the data points (observations) most suitable for parameter estimation which means that the scores matrix and not the loading matrix was the focus of the analysis.

The scores matrix and the loading matrix together form a linear combination to model the data matrix X (size $N \times K$) according to

$$X = TP + E \quad (1)$$

where (for a PCA model with A components) T (size $N \times A$) is the scores matrix, P (size $A \times K$) is the loading matrix, and E is the residual.

2.2 D-OPTIMAL DESIGN

For linear models traditional experimental designs such as full factorial designs, fractional factorial designs, and response surface designs are suitable when the factors are relatively unconstrained. For non-linear models such as a full scale catalyst, on the other hand, less traditional models such as D-optimal design may be more favorable.

If there would be restrictions on the number of experimental runs a full factorial design could be used as a candidate set (C) for D-optimal design to

create a new design matrix (X) with fewer rows (note that the candidate set can have several different origins, for example it could also be a large set of data where a high variable correlation has limited the available variable combinations). The D-optimal design algorithm would then in an iterative process select different combinations of rows from the candidate set that minimizes covariance of the new design matrix by maximizing the determinant of $X^T X$ (hence the notation D-optimal as in determinant). This would maximize the orthogonality of the design matrix and as such create the design with the best conditions for parameter estimation with the defined number of runs. Note that the iterative process in which D-optimal design is performed contains certain random factors which means that the D-optimal design performed on a large candidate set likely will generate different design matrixes on different runs.

3 EXPERIMENTAL

All experiments in the present work were performed with a full scale engine rig which also means that the catalysts used were all of commercial dimensions for heavy-duty vehicle aftertreatment systems. To use an engine as the exhaust source together with full scale catalysts results in real challenges for how the experiments should be performed. This is not only due to the fact that a full scale catalyst is a complex system but also because the engine itself severely limits the possibilities to vary the catalyst inlet conditions. In this section the different engine rig set-ups used in Paper I and II (section 3.1), and Paper III (section 3.3) are introduced together with the possibilities for experimental design made available with these set-ups. The different catalyst configurations used in the experiments are also presented.

3.1 CATALYST CONFIGURATIONS

As mentioned in the previous section the experimental design does not only include how the inlet conditions to the catalyst is controlled, the design of the actual catalyst is also a very important part. Catalyst properties such as, noble metal loading, washcoat thickness, catalyst volume, and active surface area will influence the reactions taking place in the catalyst. To achieve a variation in these properties a number of different model catalysts were custom made for the project.

TABLE 1 Properties of catalysts used in the project. Pt-loading is shown in two different units where the unit in the first column is commonly used in lab scale and the unit in the second column is commonly used at industrial scale.

Pt-loading [mass % washcoat]	Pt-loading [g/ft³monolith]	Average washcoat thickness* [mm]
0.10	5	0.110
0.30	15	0.110
0.59	15	0.055
0.59	30	0.110
1.78	90	0.110

*Washcoat thickness is generally higher in the corners of the channel and may also vary axially

The catalysts in table 1 were all made with replicates making it possible to put them in series to create catalyst configurations with increased catalyst volume and thereby also increase residence time for the exhaust in the catalyst. All catalysts were of monolith flow-through type with 62 square channels per cm² (400 cpsi), a total diameter of 30.5 cm (12 inch), and a total length of 10.2 cm (4 inch). The catalysts were platinum on alumina model catalysts and were provided by Johnson Matthey.

3.2 ENGINE RIG EXPERIMENTS

Two different experimental set-ups have so far been used in this project. The first set-up, of more traditional type, was used for both Paper I and II and the experiments were performed at Johnson Matthey in Gothenburg.

3.2.1 SET-UP

The traditional engine rig simply consists of an engine connected to the catalyst that is to be investigated. The exhaust properties are varied by controlling the engine operating point and the temperature, flow rate, and composition before and after the catalyst are measured.

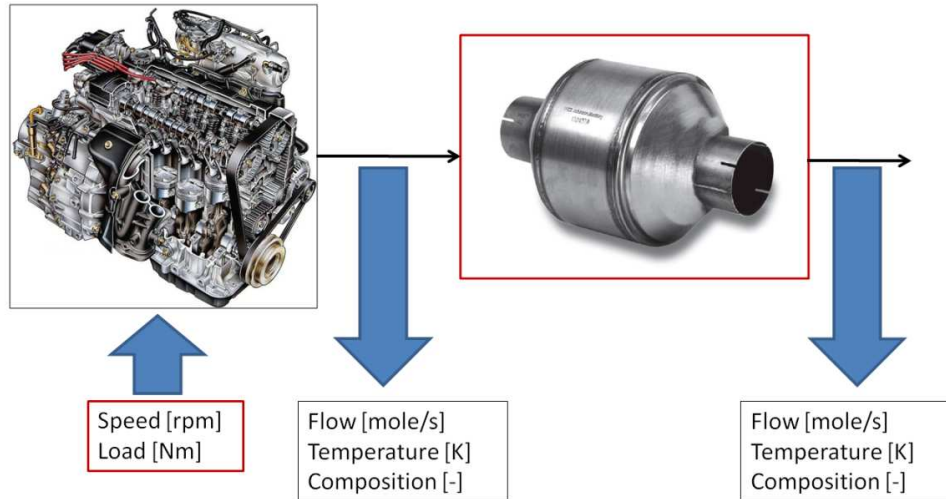


FIGURE 5 *Traditional engine rig set-up. The red frames around the catalyst and the engine operating point indicate that these are controlled by experimental design.*

A Euro IV calibrated heavy duty diesel engine with disabled exhaust gas recirculation (EGR) was used as the exhaust source and Swedish MK1 diesel, a commercial low-sulfur (less than 10 weight ppm sulfur [17]) diesel, was used as fuel. The engine was equipped with a dynamometer control system enabling independent control of load and speed.

The temperature and composition measurements were made according to figure 6 where the downstream catalyst position (Cat. 2) was left empty if only one catalyst was used.

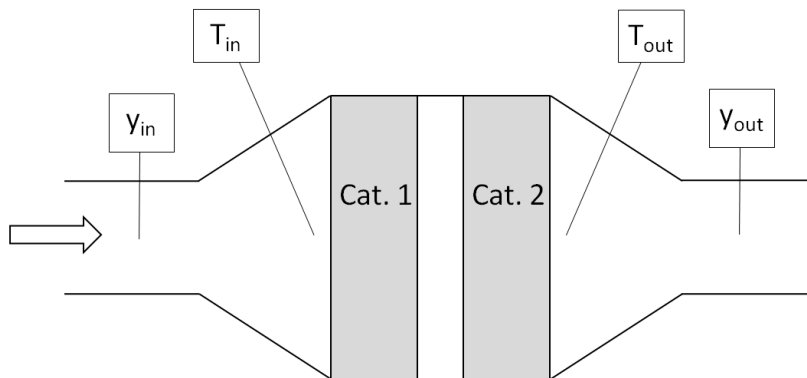


FIGURE 6 *Catalyst measurement points where T indicates temperature and y composition.*

The temperatures were measured with 3 mm thermocouples positioned at the center of the pipe and close to the catalysts. The inlet gas composition was

measured just before the pipe expansion and the outlet gas composition was measured directly downstream the pipe contraction.

3.2.2 EXPERIMENTAL DESIGN

To obtain a widespread experimental range, six different catalyst configurations with different noble metal loading, lengths, and washcoat thicknesses were used. This included all catalysts in table 1 and also one configuration where two catalysts with 0.30 wt% Pt (second row in table 1) were used in series. Of the selected catalyst configurations the ones with the highest and the lowest platinum loading (0.10 and 1.78 wt% Pt) were used for validation while the remaining four were used for parameter estimation.

As mentioned in the introduction the available exhaust composition, flow and temperature is limited by the operating points of the engine. It also takes several minutes for the catalyst inlet conditions to reach stability when switching between operating points, which means that experimental time will be a factor when deciding the number of different operating points when the full transient behavior is of interest. An important part of the current work is to investigate what experiments are suitable for parameter estimation and therefore both transient and steady-state data was desirable. Since the number of catalyst configurations was large and some replicates also were necessary only 8 different operating points were selected according to table 2.

TABLE 2 *Engine operating points and levels of variables, Med=medium.*

Number	Description				
	NO _x	HC + CO	O ₂	Temp.	Flow
1	Low	High	High	Low	Low
2	Low	High	High	Low	Med
3	High	Med	Med	Med	Low
4	Med	Low	Med	Med	High
5	High	Low	Low	High	Med
6	Med	Low	Med	Med	High
7	High	Low	Low	High	Med
8	Med	Low	Low	High	High

The operating points were selected manually but were later confirmed to be close to a D-optimal selection (see section 2.2) with a model based design analysis of the engine map in temperature, concentrations and flow. Figure 7

shows an example of how the operating points span over the engine map for the case of exhaust temperature.

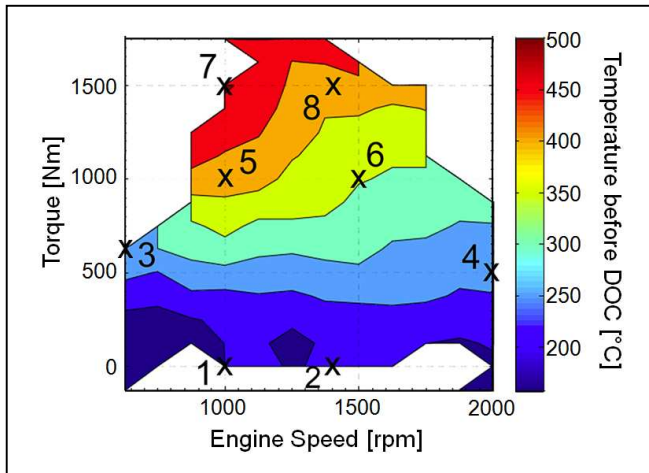


FIGURE 7 *Temperature engine map and selected operating points*

The operating points were selected to make as large steps as possible in the different variables including concentrations of NO, NO₂, HC, CO and O₂ as well as temperature and flow rate with the purpose of making the experimental space as large (and orthogonal) as possible. Some of the variables, such as concentrations of NO and NO₂ and concentrations of HC and CO, are closely correlated and it is difficult to create transients where they are changed independently. This is also the case for O₂ and temperature, i.e. an operation point with low temperature will have high oxygen concentration and an operation point with high temperature will have low oxygen concentration. This means that some of the input variables cannot be varied independently. A good experimental plan will however ensure that the variables are varied as independently as possible.

The operation points were run in the order 1, 7, 2, 8, 3, 4, 5, 6 for all catalyst configurations to make as large transient changes as possible in as many variables as possible. For some of the configurations several additional sequences were also run. To achieve steady state conditions all points were run for 15 minutes each.

3.3 SCANIA ENGINE RIG

When switching between two engine operating points it generally takes several minutes before the properties of the emissions have stabilized. The main reason is the large thermal mass between the engine and the investigated catalyst which will not only affect the transient behavior of the temperature but also of the concentrations. This not only makes the experiments time consuming, but it also complicates the transient modeling of the DOC since the changes in inlet properties are far from ideal step functions.

Kolaczkowski et al. [18] presented a method where a pollutant was injected between the studied DOC and the engine to achieve transient data without changing the engine load point. This method also presents the great benefit that the heat accumulation problem is avoided, since the engine load and thereby the temperature is constant, and thus very fast transients in concentrations can be achieved. Sjöblom [19] further extended this concept by also having the possibility to reduce the flow (increase residence time) and control the temperature.

In the Scania engine rig a set-up is presented where additional catalysts are inserted upstream of the investigated catalyst. By using different bypass settings and injection of urea the catalyst inlet composition could be changed without changing the engine operating point resulting in faster transients.

3.3.1 SET-UP

In the set-up of the Scania engine rig an extra DOC with the possibility for bypass flow and an SCR with urea injection were mounted before the investigated catalyst (DOC 2), as illustrated in figure 8.

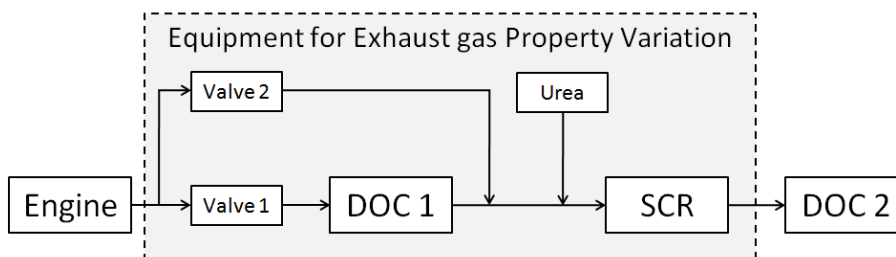


FIGURE 8 *Experimental set-up. "DOC 2" is the test object to be studied*

The fraction of exhaust gas flow through DOC 1 allows variation in the conversion of HC and CO to CO₂ and H₂O, and the conversion of NO to NO₂. By injecting different amounts of urea the conversion of NO₂ and NO to N₂ is

controlled and the ratio of NO_2 to NO_x can be adjusted, the engine was also tuned to run with late fuel injection to achieve high HC and CO concentrations. A Vanadium based commercial SCR and a commercial platinum only DOC were used for exhaust gas property variation.

3.3.2 EXPERIMENTAL DESIGN

The fast transients and the wide range of possible settings for the DOC bypass and urea injection made it possible to achieve a wide variation of exhaust compositions for every engine operating point in a short time span. Instead of searching for the best points in the engine map, the focus of the experimental design was instead put on finding the operation of the DOC bypass and urea injection that will generate the data best suited for parameter estimation.

Three different experimental types with different operation of DOC bypass and urea injection were evaluated:

1. Urea injection and SCR have been removed from the configuration shown in figure 8. Valve 1 is switching between 20% and 90% open at the same time as valve 2 is switching between 80% and 10% open every 20 seconds.
2. Set-up as in figure 8. Urea injected for 20 seconds followed by 20 seconds of no injection. Valve 1 and 2 in locked positions.
3. Set-up as in figure 8. Valve positions switching every 20 seconds. Urea injection is switched on/off every 20 seconds with a 10 s delay relative to the valve positions switching.

All experiments were run at more than 20 different engine operating points and to further expand experimental space several catalyst configurations have also been used for the same experiments.

4 MODELING

4.1 REACTOR MODEL

A full scale catalyst monolith with varying inlet properties displays a highly dynamic behavior. This means that the catalyst outlet conditions will not only be influenced by the current inlet conditions but also those at previous time points. To describe this behavior a catalytic reactor model with accumulation terms is needed. The level of detail needed in the model is of course depending on its purpose. If all details of mass, heat and momentum transport are required and computational time is not an issue then a complete 3D CFD model may be the best option. In this work the model was used for parameter estimation which means that it was used in an iterative process to fit model parameters to measurement data and as such the simulation time is also a very important factor.

Both the heat and the mass transfer in a monolith catalyst occur at a wide range of connected length scales. The channels of the monolith in this project are about 10.5 cm long and have an opening with a width of less than 1 mm. For reaction to occur the reactants first need to be convectively transported from the gas phase to the solid washcoat surface. From the surface they need to further diffuse into the washcoat (thickness around 100 micro meters) with pores that have pore diameters less than a micro meter to react on the noble metal active sites.

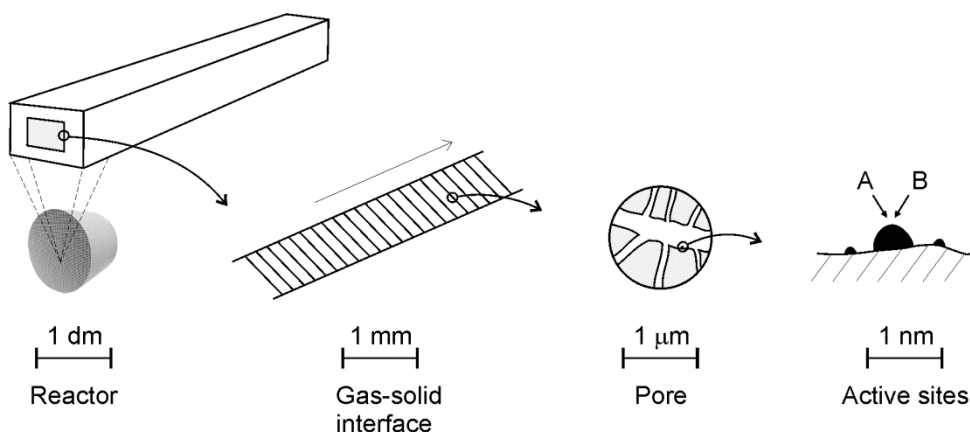


FIGURE 9 Scales of heat and mass transport in full scale catalyst.

A full scale catalyst of the size used in this project has over 40 000 channels. If all channels are to be modeled individually an extremely high resolution is needed if phenomena like concentration gradients in the washcoat (as a function of reaction rates and heat and mass transport), and radial temperature gradients are to be modeled. A model of such complexity is not feasible for parameter estimation and to reduce simulation time some significant simplifications are needed.

Since the catalyst is cylindrical and thereby symmetrical around the axial axis it would be possible to simplify the model by only modeling one row of channels in the radial direction. A full scale catalyst with the specifications given in section 3.1 has a radial distance spanning 120 catalyst channels and the computational demand would be reduced with more than 2 orders of magnitudes if an axisymmetrical modeling approach is taken. The flow upstream of the catalyst is however turbulent which means that a one dimensional description of the heat and mass profile will not be able to fully replicate the true conditions. A model consisting of 120 catalyst channels is still a very complex system if modeled in three dimensions. A model with good accuracy would therefore be too computationally demanding to be used for parameter estimation, likely the simulation time would be in the range of hours to days and not minutes to hours [20].

The two significant transport phenomena for a full scale catalyst model are heat and mass. The mass transport is limited by the solid substrate walls meaning that the mass entering one channel is also leaving the very same

channel. The distance from the engine to the catalyst is long and turbulent enough to be considered well mixed and thus the composition in the inlet to all channels can be assumed to be roughly the same. Heat can be transported between the channels through the solid material in the catalyst which makes the heat transport within the catalyst clearly different from the mass transport. There will also be heat losses to the environment both in the piping leading to the catalyst and from the catalyst itself meaning that there will be radial temperature gradients both in the catalyst inlet and inside the catalyst. In [21] a method was presented where a full scale CFD-based model was used to solve the 3D temperature profile in the catalyst which in turn was coupled to a simple 1D model for reactions in the catalyst washcoat. A similar approach is taken by Stamatelos et al. [22] but the solid energy balance is solved for an axisymmetric 2D model.

The general trend for simulation of monolith converters is however still significantly simpler 1D models for both heat and mass [23] where all channels are assumed to have the same inlet conditions, heat loss (if any), and flow rate. The advantage with these kinds of models is of course high simulation speed and the drawback is reduced accuracy [24].

In this work a 1D/2D single channel model, closely based on the model presented by Ericson et al. [25], was chosen since it was considered a good compromise between accuracy and computational speed [26]. Due to surface tension effects during the washcoating process the washcoat usually is thicker in the corners of the channel and thinnest furthest from corners. In the current work the washcoat formulation has however been simplified to a slab representation with constant washcoat thickness to avoid the need of a third dimension to model the washcoat.

The gas phase in the channel was assumed to have fully developed laminar properties which and thereby a discretization in the axial direction only (1D) was assumed to be sufficient if combined with a film transport model for the gas bulk interface. The wide temperature range of vehicle exhaust together with the need to package as much activity into a given volume of the converter as possible to achieve vehicle on-board space-efficiency, leads to transport limitations usually becoming unavoidable. This means that large gradients in

the washcoat are likely to occur which makes the washcoat discretization specifically important for a proper description of the behavior of the system. The washcoat was therefore chosen to be discretized both radially and axially (2D), see figure 10. The method used for discretization was tanks in series mainly selected for its robust properties in transient simulations. A film theory model was used to model the heat and mass transport between gas and washcoat surface.

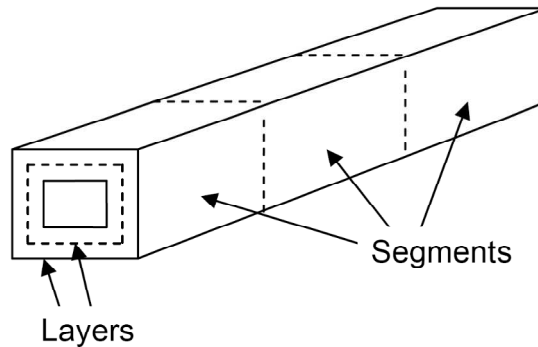


FIGURE 10 *Illustration of the catalyst discretization principle of a single channel*

As have already been mentioned there are some clear differences between heat and mass transfer and the modeling of the different phenomena will be described separately below, for full details see Paper I.

4.1.1 MASS TRANSPORT

For every tank and species the balance $\{in\} - \{out\} \pm \{produced\ or\ consumed\} = \{accumulation\}$ is made. In the gas bulk no reaction takes place which means that the balance only includes convective transport with the flow and transport to and from the washcoat. The diffusive transport in the gas bulk in the axial direction is not taken into account in the mass balance since it is considered negligible compared to the convective flow.

The transport resistance between the gas bulk and the first washcoat layer is modeled as two parts; firstly it is the film transport resistance and secondly it is the diffusive transport resistance of half the washcoat layer thickness. This configuration is chosen since it will represent the concentration in the centre of the washcoat layer and thus a good estimate of the average concentration in the volume represented by the tank. Only the asymptotic value for the Sherwood number was used to calculate film transport resistance and thus entrance effects were neglected. Asymptotic values were taken from [27].

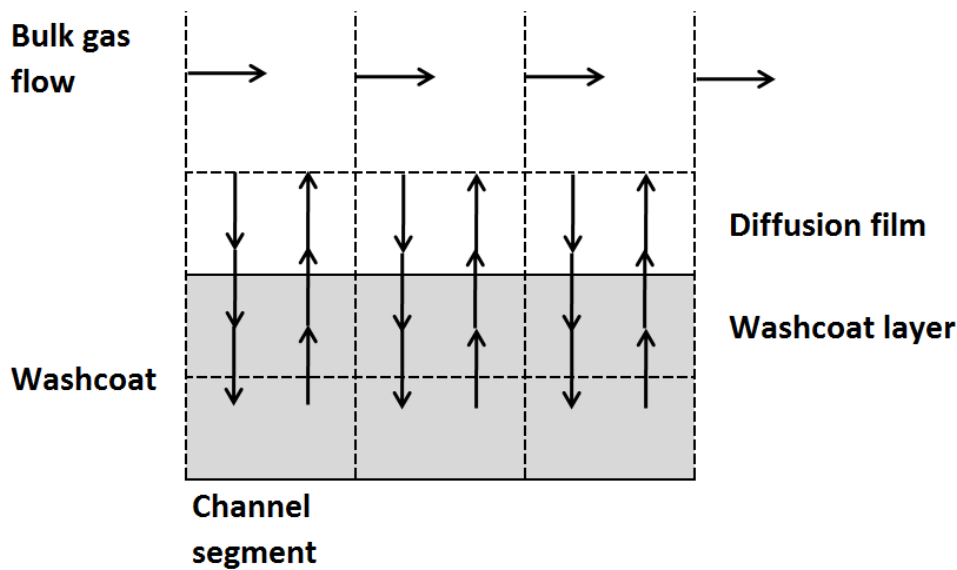


FIGURE 11 *Mass transport discretization*

For further transport in the washcoat the resistance is also consisting of two parts which are the diffusive resistances of half the washcoat thickness of both layers. The axial transport in the washcoat is neglected since the axial transport distance is about 3 orders of magnitude larger than the radial transport distance. If a very large segments to layers ratio (see figure 10) would be used this simplification may need to be reconsidered. A description of the mass transport in the washcoat and its discretization is shown in figure 11.

The model will have a very dynamic behavior which means that accumulation terms are needed for an accurate description. Accumulation terms do however generate a significant increase in the computational cost and if the transient time scales are small the model stiffness and instability may increase. Accumulation terms should therefore be carefully analyzed before included in the model. In the case of gas phase concentration, the characteristic time constants are low which means that a new steady state point will be reached within tenths of a second if the inlet concentrations are changed at constant temperature (see section 6.3 for example). The characteristic time constant for temperature is, on the other hand, large and will dominate the dynamic behavior of the model and as a result accumulation of gas phase species both in the gas bulk and in the washcoat are neglected. In micro kinetic models the adsorbed species influence all reaction rates and are also important

accumulation terms. In the kinetic model used in the current study the adsorbed species dependence is modeled by an inhibition term only as a function of temperature and the washcoat concentrations. The transient behavior of the adsorbed species is thereby not described by an accumulation term (the inhibition term is independent of previous temperature and concentrations) which will make the kinetic model less suitable to describe transient behavior.

It should be noted that these simplifications were made for the modeling from data generated by the experimental methods in the traditional engine rig (section 3.2) where temperature, flow and species concentration cannot be changed independently. For modeling of data generated by the Scania engine rig set-up where the temperature is relatively constant the same simplifications may not be applicable.

4.1.2 HEAT TRANSPORT

The modeling of the heat transport in the gas bulk is analogous to the mass transport in the gas bulk; the discretization is only made axially, the thermal conduction is neglected, and the film resistance is calculated from an asymptotic value for the Nusselt number [27]. The modeling of the heat transport in the washcoat on the other hand displays several differences from how the mass transport was modeled. The main difference originates from the fact that the heat transport resistance is much lower (high heat conduction) than the mass transport resistance (low effective diffusivity).

For the mass transfer modeling the long axial transport distance coupled with the high transport resistance meant that axial mass transport in the washcoat was neglected. In the case for heat transport the long axial distance is counterbalanced by the low transport resistance which means that axial heat transport cannot be neglected. The efficient heat transport in the washcoat also means that transport in the significantly shorter radial direction will be very efficient and as a result the radial heat transport resistance was neglected. Neglecting the radial heat transfer resistance means that the radial discretization of the washcoat that was necessary for mass transfer can be simplified to a single layer for heat transport. An illustration of the discretization can be seen in figure 12.

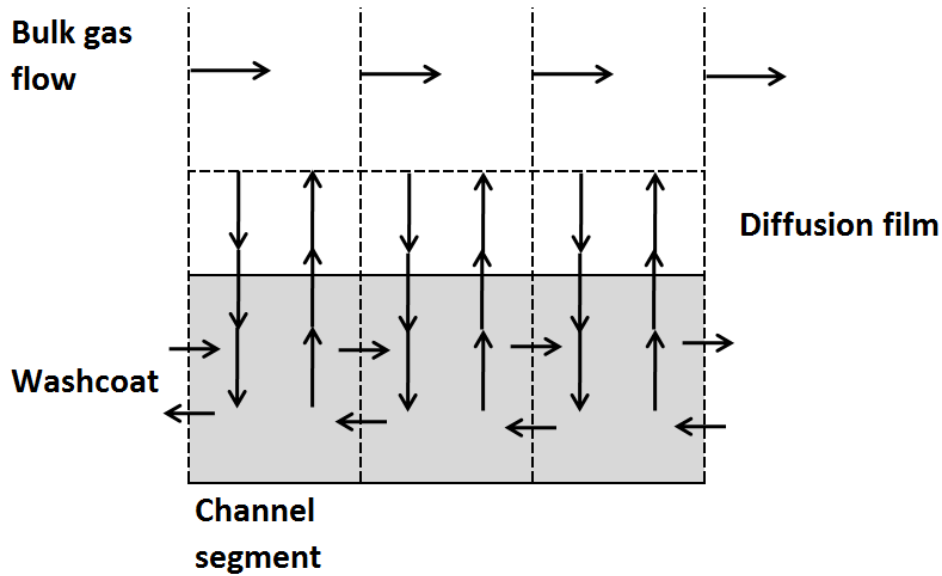


FIGURE 12 *Heat transport discretization*

The efficient heat conduction in the washcoat and substrate means that phenomena like heat loss to the environment and heat accumulated in surrounding materials such as insulation and canning will have a large influence on the behavior of the monolith if adiabatic conditions do not prevail. Since only one channel is modeled a heat loss term and extra heat accumulation term is added to every washcoat channel segment to model the two aforementioned phenomena. Modeling the heat loss to the environment as equal for all channels is a rough simplification but the alternative of modeling more channels with different temperatures and heat losses was considered to require a too large increase in computational demand.

4.1.3 DISCRETIZATION

The number of segments and layers are of utmost importance for the performance of the model. A too low number of segments and layers will make the simulation dependent on the discretization and a too high number of segments and layers will lead to unnecessarily long simulation times. For the parameter estimation performed in this project a model discretized as 10 (axial) segments and 8 (radial) layers was considered a good tradeoff between model accuracy and simulation time. It should be noted that the number of axial segments is lower than what is theoretically necessary to model a tube

reactor [28] with the current dimension and experimental data, which will result in an over representation of axial dispersion.

A major influence on the model performance is not only the number of segments and layers but also how they are distributed. In general the faster a property changes in one direction a finer discretization is needed to fully resolve a concentration or temperature gradient. For a catalyst at high temperature, the reaction rate will be high which means that some components may be consumed before they have diffused radially through the washcoat. Also, the fact that diffusive flux of all components is set to zero at the washcoat-carrier material interface means that concentration gradients will approach zero close to the carrier material and be steeper at radial positions close to the surface. In other words a fine discretization close to the washcoat surface would be needed but not close to the carrier material. At low temperatures the reaction rate will be slow and concentration will not change much with radial position and thus there is little need for a fine radial discretization. With this in mind, a washcoat discretization that decreased linearly with radial position was chosen which is demonstrated for eight layers in figure 13.

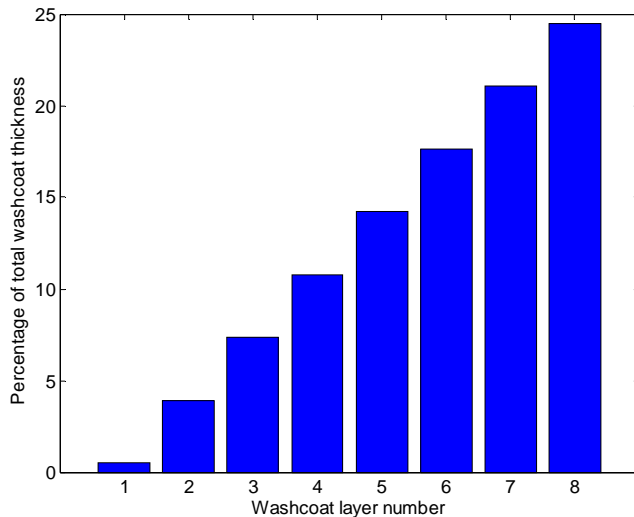


FIGURE 13 *Radial washcoat discretization for eight layers*

For axial discretization the same reasoning can be applied as for radial discretization; it is more likely that the axial gradients are larger close to the inlet than close to the outlet. This indicates that a discretization decreasing with axial position would be preferable also in this direction. However, a

conversion close to 100% - which would be the case for a steep concentration gradient close to the inlet is not generally desired since these kinds of experiments are less informative in a kinetic parameter estimation point of view. The dynamic behavior of the model also means that different parts may experience large gradients at different conditions. For example when the inlet temp is changing from high to low the outlet end of the monolith can have a higher temperature than the inlet end and as a result gradients can be steeper near the outlet. With this in mind an equidistant axial discretization was selected.

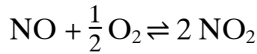
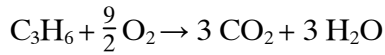
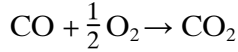
4.2 KINETIC MODEL

Large efforts have been made to construct kinetic models for the DOC both of global type [11, 29-31] and microkinetic type [32-34]. The microkinetic models describe all reactions divided into elementary steps, which makes it possible to derive estimated kinetic parameters from reaction rate theory. In the global models the elementary steps are assumed to be either rate-determining or in equilibrium, which makes it possible to derive rate expressions for the overall reactions with a significantly reduced number of parameters compared to the microkinetic models [35]. These global rate expressions generally use only gas phase concentrations which are also used to account for inhibition, adsorption and desorption. However, since catalytic reaction mechanisms are often not understood down to the elementary step level the global rate expressions are rarely strictly derived from elementary reaction steps. Instead, they are often adjusted and sometimes expanded with additional semi-empirical expressions to better describe observed experimental data. In addition, reaction steps may be neglected and parameter values lumped all with the aim of reducing the kinetic model complexity and number of adjustable kinetic parameters. These kinds of simplifications and modifications of rate expressions may also lead to the kinetic parameters having less of a physical nature and more importantly becoming more case-specific and less generally applicable [35]. Nevertheless, the far lower computational demands of global kinetic type models means that they are often the model-type of choice for aftertreatment design evaluations and control algorithms. It should be noted that exclusion of adsorbed species in the global models will make them less suitable to describe transient

behavior, see section 4.1.1, even though it may not be an issue for species with low surface coverage.

The simplest versions of the DOC kinetic models only describe the oxidation reactions of CO, HC, and NO. In addition HC is often represented as one molecular species, usually propene [11, 36, 37]. The exhaust composition is far more complex than just one type of hydrocarbon species and there are examples of kinetic models [22, 29] that have been expanded with several types of HC. Other additional reactions that may be added are H₂ oxidation [22, 34] and HC reduction of NO_x [30, 38] or by NO₂ [29]. In this work rather than focusing on the required model formulation or level of detail of the kinetic model, it was the method used to estimate kinetic parameters for a given kinetic model that was in focus.

The kinetic model used in this study is of Langmuir-Hinshelwood type and was originally suggested in the classical work by Voltz et al [11] and later modified by Oh and Cavendish [36]. The model, which has been widely and frequently used in DOC modeling over the years, only includes three reactions of which one is an equilibrium reaction:



The reaction rates were calculated according to equations 2 to 6.

$$r_1 = \frac{k_1 y_{\text{CO}} y_{\text{O}_2}}{G(y_i, T_s)} \quad (2)$$

$$r_2 = \frac{k_2 y_{\text{C}_3\text{H}_6} y_{\text{O}_2}}{G(y_i, T_s)} \quad (3)$$

$$r_3 = \frac{k_3 y_{\text{NO}} y_{\text{O}_2}}{G(y_i, T_s)} \left(1 - \frac{K'}{K_p} \right) \quad (4)$$

$$K' = \frac{y_{\text{NO}_2}}{y_{\text{NO}} y_{\text{O}_2}^{1/2}} \quad (5)$$

$$G(y_i, T_s) = T_s \left(1 + K_4 y_{CO} + K_5 y_{C_3H_6} \right)^2 \left(1 + K_6 y_{CO}^2 y_{C_3H_6}^2 \right) \left(1 + K_7 y_{NO}^{0.7} \right) \quad (6)$$

where K_j is the reaction rate coefficient for the inhibition terms in the denominator G and K_p is the equilibrium constant for NO oxidation. At thermodynamic equilibrium, K_p will be equal to K' and reaction rate r_3 will be equal to zero. Both reaction rate coefficients k_j and K_j were described by Arrhenius expressions:

$$k_j = A_j e^{-\frac{E_{A,j}}{RT_s}} \quad (7)$$

The start values for estimation of kinetic parameters were taken from Wang et al. [37] where results from several studies [39-45] were compiled. The initial values for kinetic parameter estimation used in this study are shown in table 3.

TABLE 3 *Start values for kinetic parameters estimation.*

Index	Pre-exponential factor [mole K/(m²s)]	Activation energy [kJ/mole]
j	A	Ea
1	1.00×10^{17}	80.0
2	4.00×10^{20}	100.0
3	4.50×10^{14}	70.0

Index	Adsorption pre-exponential factor [-]	Adsorption activation energy [kJ/mole]
j	A	Ea
4	65.5	-8.0
5	2080	-3.0
6	3.98	-96.5
7	479000	31.0

The kinetic parameters in equations 2 to 6 are highly correlated and since the parameter values in table 3 were taken from different studies, the fit of the model to experimental data was expected to be poor before any parameter tuning was performed. However, the parameters were successfully used as a starting point for parameter tuning of a DOC against engine rig data by Wang et al. [37] which was also the intended application in the present work.

5 PARAMETER ESTIMATION

With the experimental plan carried out, the catalyst and kinetic models selected, the parameter estimation can finally be performed. The standard procedure of parameter estimation for automotive catalysts is to use all experimental data points to estimate kinetic parameters only. In the current project the estimation of kinetic parameters are complemented by estimation of heat and mass transport parameters to better describe the dynamic behavior of the full scale catalyst. A method of decreasing parameter estimation time by reducing the number of data points by Multivariate Data Analysis (MVDA) was also evaluated (Paper II).

5.1 ADJUSTABLE PARAMETERS

At lab scale the heat losses to the environment can usually be kept at negligible levels (insulation or heating of the monolith are two common measures) and also the mass transport resistance can be reduced by using thin washcoat layers or even using powder of crushed monolith [46]. In the case of full scale catalysts heat- and mass transfer limitations are more likely to have an important influence on the results, as has been discussed above. The parameters affecting the heat- and mass transfer resistance are difficult to measure and the best option may be to instead use simplified models where a few parameters are tuned to experimental data.

The parameter estimation is performed with parameters in scaled and centered forms [47]. Which means that the estimated parameter is equal to an original value from literature or previous estimation plus/minus the adjustable

parameter, p , times a weight factor, w . For example the activation energy is estimated by

$$E_{A,j} = E_{A,j}^o + w_{Ea,j} p_{Ea,j} \quad (8)$$

where the superscript “o” indicates that this is the original value. The value of the weight factor is selected to make the sensitivity of the residual sum of square on the same order of magnitude for all estimated parameters.

5.1.1 KINETIC PARAMETERS

All the pre-exponential factors, A_j , and activation energies, $E_{A,j}$, determining the reaction rate coefficients in equations 2-6 have been tuned to experimental data. It should here be stressed that the parameter estimation is a retuning of kinetic parameters determined at lab scale and not estimation of parameter values based on theoretical considerations. The starting point of kinetic parameter estimation will therefore be the values in table 3.

The parameter estimation of activation energies has already been shown in equation 8 and is straight forward. The parameter estimation of pre-exponential factors is performed in three steps [48]. As a first step the reaction rate coefficients are centered on a reference temperature with the purpose of reducing the correlation between activation energies and pre-exponential factors.

$$k_{j,ref}^o = A_j^o e^{-\frac{E_{A,j}^o}{RT_{ref}}} \quad (9)$$

With the performed centering the activation energies will capture the temperature dependence and the pre-exponential factors will capture the amplification. The reaction rate coefficient $k_{j,ref}$ is scaled according to

$$\ln(k_{j,ref}) = \ln(k_{j,ref}^o) + w_{a,j} p_{a,j} \quad (10)$$

The tuned rate constant at a reference temperature is then used to calculate the pre-exponential factor

$$A_j = k_{j,ref} e^{\frac{E_{A,j}}{RT_{ref}}} \quad (11)$$

When equation 11 is inserted into the expression for the reaction rate coefficient in equation 7, the following expression for the tuned reaction rate coefficient is obtained

$$k_j = k_{j,ref} e^{-\left(\frac{E_{A,j}}{R} \left(\frac{1}{T_s} - \frac{1}{T_{ref}}\right)\right)} \quad (12)$$

It has been shown that the catalyst active surface area could be used as a single parameter in a global model [49]. In addition to the pre-exponential factors and the activation energies, an activity scaling factor has therefore also been selected as an adjustable parameter. The activity scaling factor is simply a scale factor for all reaction rates on a certain site on a certain catalyst (parameters were tuned to several different catalyst samples simultaneously). This means that the catalyst active surface area was tuned for each catalyst sample since only one single site is used in the kinetic model.

5.1.2 HEAT TRANSPORT PARAMETERS

The heat loss term and extra heat accumulation term that was added to every washcoat channel segment in the model (see section 4.1.2) represent two parameters that are difficult to measure. Instead these parameters were fitted to measurement data together with an environmental temperature.

The temperature in the catalyst has a very large influence on the reaction rates and conversion of the different components. For a full scale DOC in an engine rig the influence on the temperature from the reaction rate will be of less significance mainly since the concentrations of reacting species is low. To be able to perform a good parameter estimation of kinetic and mass transport parameters it is therefore important to have good accuracy in the heat transfer model but not necessarily the other way around. With this in mind the heat transport parameters were estimated before the other parameters which meant that original parameter values were used for kinetic- and mass transport parameters. By estimating the heat transport parameters separately the high correlation between reaction rates and heat transport parameters is reduced. When the heat loss parameters are estimated it will be against the residual of outlet temperature alone and when kinetic- and mass transport parameters are estimated it will only be against concentration residuals. The risk that heat

transport parameters are estimated to improve the fit of outlet concentrations is thereby avoided.

5.1.3 MASS TRANSPORT PARAMETERS

In a system where both mass transport rate limited and reaction rate limited conditions will prevail the transport in the washcoat will be of great importance for the behavior of the catalyst system as a whole. The transport resistance in the washcoat is influenced by the diffusivity at different length scales and the structure of the washcoat. Several different correlations are available to determine the diffusivities but the influence of the washcoat structure is more complicated to identify. In this study the transport resistance in the washcoat has therefore been tuned with the aim of reducing the correlation between mass transport and kinetic parameters. The method used is presented below.

The species used in the kinetic model are O₂, NO, NO₂, CO, and HC which means that these also are the species whose mass transport is significant for the behavior of the model. In the catalyst model presented in [50], on which the current catalyst model is based, an expression for the effective diffusivity was derived according to

$$D_{eff,i,k} = \frac{f_D}{\frac{1}{D_{i,k}} + \frac{1}{DK_{i,k}}} \quad (13)$$

Where f_D is a factor that takes into consideration the porosity and the tortuosity of the porous material, $DK_{i,k}$ is the Knudsen diffusivity, and $D_{i,k}$ is the gas diffusivity.

This expression describes the transport resistance in the catalyst washcoat but provides only a rough estimate. Firstly the f_D factor itself should account for both the tortuosity and the porosity of the washcoat by just one constant which makes it difficult to estimate. Secondly the structure of the pores may contain cracks and other discrepancies which would make the resistances in parallel suggested by the model (denominator of $1/D_{i,k}+1/DK_{i,k}$ in equation 13) far from reality.

The mass transport was tuned by adjusting a scaling factor for the effective diffusivities for the species taking part in the reactions.

$$f_{D_{scale,i}} = f_{D_{scale,i}}^o + w_{D_{scale,i}} p_{D_{scale,i}} \quad (14)$$

This will change the expression for the effective diffusivity according to

$$D_{eff,i,k} = \frac{f_D}{\frac{1}{D_{i,k}} + \frac{1}{D_{K,i,k}}} f_{D_{scale,i}} \quad (15)$$

The value for $f_{D_{scale,i}}^o$ is typically around 1.

The species were divided into two groups, where the first group contained O₂, NO, NO₂, and CO and the second group contained HC. In the first group all species are well defined with similar diffusivities and could be expected to have similar mass transport properties in the washcoat with presumably the same bias from their true values. To reduce the number of parameters to tune, the same scale factor was used for all species in this group. The second group contained HC which was represented as C₃H₆ but in reality is a wide range of hydrocarbons with different mass transport properties. The scale factor for the second group was in other words expected to be influenced both by the hydrocarbon composition and the washcoat structure while the scale factor for the first group mainly accounted for only washcoat structure.

5.2 STANDARD METHOD OF PARAMETER ESTIMATION

The most common way to perform parameter estimation is probably to use all time points in the data to which the model is to be fitted by applying a gradient search method algorithm. This method was used in Paper I as a reference to compare to the results from Paper II where parameter estimation with PCA and D-optimal Design was used together with the same gradient search method.

5.2.1 GRADIENT SEARCH METHOD

Several different optimization methods can be used to minimize the simulated residuals and the most common method is probably the gradient search method which was also the method used in this study. The method is very efficient for linear systems but can also be applied for non-linear systems such as catalyst models. For a non-linear system the residual function is first

linearized for all parameters (the resulting matrix is known as the Jacobian, see section 5.3.1) and then a step in the parameter space is made in the direction of the steepest descent. This process is repeated until the change in residual is below a certain tolerance. The method is thoroughly described in, for example [13], but a short description of how the step in parameter space is calculated will also be given here.

The functioned to be minimized is the residual sum of squares according to

$$\min_{\beta} f(x, \beta)^2 = (y_{\text{observed}} - y_{\text{model}}(x, \beta))^2 \quad (16)$$

where x is the variables, β is the parameter values and y is the measured and simulated responses. If a specific set of data is considered the variable dependence can be dropped and equation 16 can be rewritten according to

$$\min_{\beta} S(\beta) = \|y_{\text{observed}} - \eta(\beta)\|^2 = \|z(\beta)\|^2 \quad (17)$$

To calculate the size of a step taken in parameter space the objective function, $S(\beta)$, is first approximated by a Taylor expansion:

$$\begin{aligned} S(\beta) &\approx S(\beta^0) + \left. \frac{\partial S(\beta)}{\partial \beta} \right|_{\beta^0} (\beta - \beta^0) \\ &\quad + (\beta - \beta^0)^T \left. \frac{1}{2} \frac{\partial^2 S(\beta)}{\partial \beta \partial \beta^T} \right|_{\beta^0} (\beta - \beta^0) = \\ &= \left\{ \begin{array}{l} \omega = \left. \frac{\partial S(\beta)}{\partial \beta} \right|_{\beta^0} \\ \Omega = \left. \frac{\partial^2 S(\beta)}{\partial \beta \partial \beta^T} \right|_{\beta^0} \\ \delta = \beta - \beta^0 \end{array} \right\} = S(\beta^0) + \omega \delta + \delta^T \frac{1}{2} \Omega \delta \end{aligned} \quad (18)$$

The approximation of $S(\beta)$ described in equation 18 will have a minima when the gradient is zero:

$$\omega + \Omega \delta = 0 \quad (19)$$

which gives the parameter step size according to $\delta = \Omega^{-1} \omega$. For the function $S(\beta) = (y - \eta)^T (y - \eta)$ the gradient ω and Hessian Ω is given by

$$\omega = -2J^T z$$

$$\Omega = 2J^T J - 2 \frac{\partial J}{\partial \beta} z$$
(20)

When setting the second term of the Hessian to zero the Gauss-Newton method is obtained where the parameter step size is only depending on the Jacobian J and residual z .

It is worth noting that the linearization of the system is the most time consuming part of the gradient search method. The effect of small steps in all directions (parameter values) must be calculated by the catalyst model for all time points before a step in the steepest decent can be made. For every step made, the catalyst model will in other words be called $p+1$ times where p is the number of parameters that are to be estimated.

The gradient search method in this work was the trust-region-reflective method [51]. This is the standard method for over determined non-linear least square problems in Matlab, the software used in this project. This method is implemented in the Matlab function `lsqnonlin`.

5.2.2 RESIDUAL WEIGHTING

When parameter estimation is performed according to the gradient search method the target function is to minimize the residual sum square. In the case of kinetic- and mass transport parameters the residuals will be calculated from the concentrations in the outlet. The species used in the model are O_2 , NO , NO_2 , CO , and HC which are, of course, all measured at the outlet of the catalyst. The relative change in O_2 molar fraction over the catalyst is however small, the diesel engine runs with oxygen excess, and is close to the noise level of the detector. Oxygen is also consumed in all oxidation reactions modeled and does thereby not add any extra information on the specific reactions. To avoid unnecessary uncertainties, the oxygen residual was not used for parameter estimation.

The molar fractions of NO , NO_2 , CO , and HC at both catalyst inlet and outlet differ by more than one order of magnitude at some engine operating points. To equalize the influence from the different species on the residual sum square, the residuals of the different species need to be weighted. The

weighting method of choice in the current study (Paper I and II) has been the inverse of the average outlet molar fraction for the different species calculated over the entire data series.

5.3 PARAMETER ESTIMATION AIDED BY PCA AND D-OPTIMAL DESIGN

The traditional way of performing parameter estimation generally gives good results since all experimental data is used but there are some drawbacks such as, long simulation time, risk of finding a local minima far from the global minima, risk of being dominated by certain parameters, and high parameter correlations. The method with MVDA described in the current work is applied to reduce these drawbacks but with similar or better end results than for the traditional method. The methodology is an extension of the work in [47].

5.3.1 METHOD

The method used for parameter estimation with the MVDA method is an iterative process divided into a number of sub-operations that are schematically summarized in figure 14.

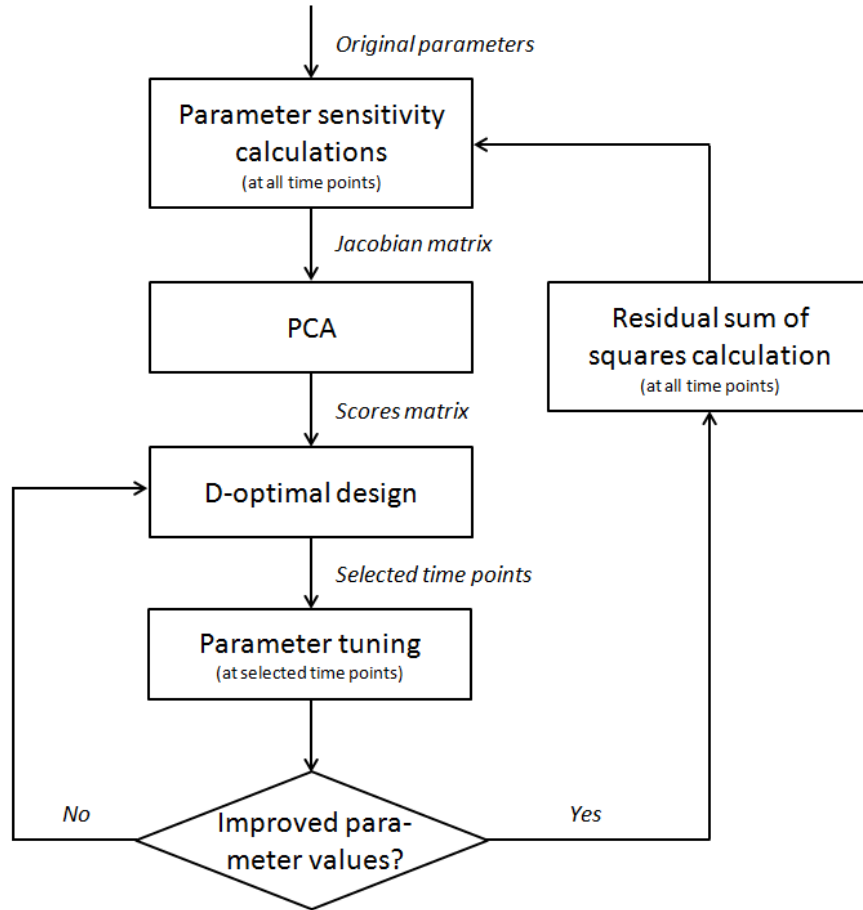


FIGURE 14 Summary of the MVDA method of parameter estimation

The first step in the method is the calculation of the parameter sensitivity matrix, often referred to as the Jacobian (J). The jacobian is defined as

$$J(f, \theta) = \frac{\partial f}{\partial \theta} \quad (21)$$

where f is the residual between simulated and experimentally measured concentration, and θ is the parameter vector in the non-linear model. The number of columns in J is different depending on applications. For use in parameter estimation with gradient search method (see section 5.2) the size of J is $[N \times k \times p]$, since the parameter sensitivity is (inherently) assumed to be based on independent responses. p is here the number of parameters, N is the number of observations and k is the number of responses (residual types). In this study the responses are correlated (eg NO and NO_2). By arranging the Jacobian as $[N \times k \times p]$ the correlation structure can be better accounted for in the D-optimal selection based on PCA, as described below.

When starting simulations with the catalyst model the only known conditions are those of the inlet and outlet flow. This means that initial conditions such as concentrations and temperature inside the catalyst need to be appraised which results in the first seconds of every simulation being unreliable. To avoid parameters being tuned against simulation results that are not reliable the first 120 s of every experimental data set was removed from the Jacobian matrix before being treated with PCA in the next step of the method.

PCA is applied to the reduced Jacobian matrix and a scores and a loadings matrix is calculated according to section 2.1 and equation 1. The resulting scores matrix will contain information about the relation between the time points and the loadings matrix will contain information about the relation between the residuals. By analyzing the scores matrix it is possible to identify time points having a large influence on the different residuals and thereby would be good candidates to retain if the number of time points used for parameter tuning were to be reduced. Several different methods for doing this kind of analysis exist and in this study the D-optimal design method has been applied.

A system of such complexity as a full scale monolith will display non-linear behavior which may result in a variable sensitivity for the selected time points when the parameters deviate from the values used for the Jacobian calculation. Adding the interaction and square terms to the scores matrix will mean that it is possible for the D-optimal design algorithm to select time points highlighted by their non-linearity. Before applying D-optimal design on the scores matrix (T) it is expanded with interaction and square terms, in order to handle the sensitivity variability described above. The D-optimal design algorithm selects rows (time points) from the expanded scores matrix (T_{exp}) that maximizes the parameter sensitivity volume (eg. the determinant of $(T_{\text{exp}})^T T_{\text{exp}}$) where the number of selected rows is chosen to be equal to the number of columns in T_{exp} . By this algorithm the time points with the most influence on the change in determinant (highest sensitivity) are identified. The main advantage of applying D-optimal design on the scores matrix instead of the full Jacobian is that the calculations of the design matrix will be much faster (roughly 5

minutes instead of 15 hours on one processor core on a standard desktop computer for the current set of data) if the number of columns is 50-200 instead of about 3000 which would have been the case if the Jacobian matrix was expanded with interaction and square terms.

With the time points identified with D-optimal design, a parameter estimation with the gradient search method is performed using the selected time points only.

Since the properties of the Jacobian matrix will be dependent on the actual parameter values the best selection of time points for parameter tuning will change as the parameters are tuned. To make the parameter tuning efficient it is therefore necessary to select new time points for parameter tuning as new parameter values develop. In the current study the time point selection with PCA and D-optimal design is followed by a period of parameter tuning that will result in new parameter values and thereby a new time point selection by the PCA and D-optimal analysis. The parameter tuning will be limited to only a few iterations (1-5) in the parameter space which will decrease the risk of obtaining a too large influence from the selected time points on the overall fit. Already after the first step in the parameter space the sensitivity may have changed significantly.

If no improved parameter values were found (resulting in a reduced residual) with the gradient search method, which is may occur since just a few steps are taken, a new D-optimal design will be performed. Even though the scores matrix is unchanged (since the parameter values are unchanged) the D-optimal design is likely to select different time points since the selection of a design matrix with D-optimal design contains certain random factors. This process where new time points are selected with D-optimal design will be repeated until parameter values can be found that reduce the residuals in the points selected. The improved parameter values will then be used to calculate the residuals on the whole data set and the parameter estimation cycle may be halted if certain criteria are fulfilled. If the criteria are not fulfilled a new sensitivity calculation on the whole data set (Jacobian matrix calculation) will be performed and the cycle is thereby back at the first square in figure 14.

5.4 COMPUTATIONAL EFFICIENCY

Parameter estimation on highly dynamic systems such as a full scale catalyst is a computationally demanding process. The focus of the project is to evaluate different methods of parameter estimation and to make them as efficient as possible which means that a lot of computational power has been needed. Without an efficient use of the computational resources available the project would simply not be where it is today. The measures taken to improve the computational efficiency are described in the following sections.

5.4.1 PARALELLIZATION

The software used for all simulations, parameter estimations, and data analysis is the well known numerical computing environment Matlab including Matlab Statistical toolbox and Matlab Parallel Computing toolbox.

The default setting for Matlab is to perform calculations on a single processor core which, in the case of a multi-core computer, means that the full computational power is not used. Matlab Parallel Computing toolbox, however, makes it possible to run computations in parallel on up to twelve processor cores, sometimes referred to as workers, on one local computer.

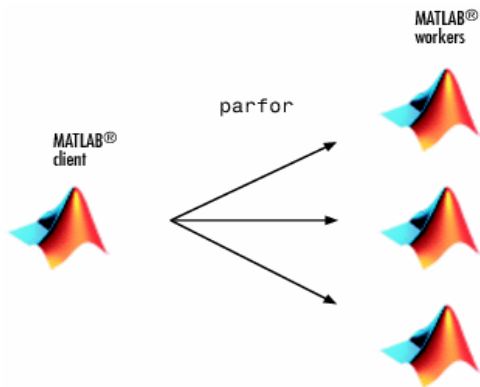


FIGURE 15 A Matlab computation can be distributed over several processor cores (workers) by creating a parfor loop

To make parallel computation possible the computations performed on each core need to be independent of the calculations on the other cores. For example it would not be possible to calculate the washcoat concentration of NO on one core and the washcoat concentration of CO on another core since both concentrations will influence each other's rate of reaction.

One set of independent calculations are simulations performed on different sets of experimental data, for example experiments on different catalyst configurations. This kind of parallelization over experiments has made parameter estimation according to figure 16 possible.

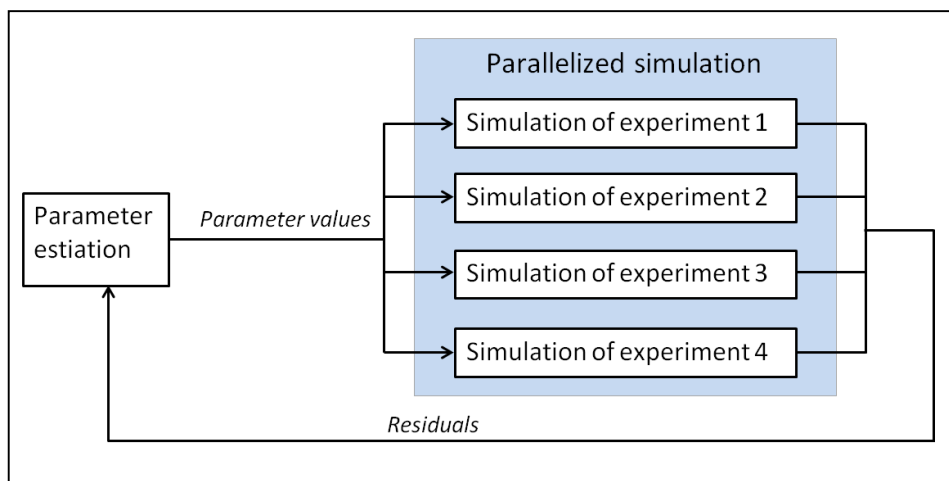


FIGURE 16 *Parallelized computation during parameter estimation illustrated by parallelization over four experiments*

The number of experiments can exceed the number of cores used in a parallelized calculation but there is no gain in having more cores available than the total number of experiments. If the experiments include about the same number of time points and have similar dynamic behavior, their simulation time should be approximately equal and thus the relative reduction in total simulation time would be of the same order as the number of cores used.

The relation between number of experiments and cores is of high importance for the computational efficiency and should be carefully considered when planning simulations if the number of core hours (hours of computational time per core) used is an issue. For example if the simulation time for one experiment is considerably longer than for the other experiments maybe they can all be sequentially simulated on one core in the same time as the long experiment is simulated on another core; two cores only would then be the most efficient use of computational resources. The fastest way to simulate is however always to have the same number of cores available as the number of experiments and when possible this configuration has been used in the current work. The theoretical increase in simulation speed on one computer is then twelve times the computational speed on one core but due to

differences in simulation time for different experiments, the practical increase in computational speed is closer to half that value.

5.4.2 CLUSTER COMPUTATION

The available desktop computer in this project has four processor cores which is what can be considered standard for computers today. On a cluster more processor cores per computer is available and there's also a possibility to perform calculations on more than one computer at once.

With the MVDA parameter estimation method, described in section 5.3, parameter estimation is performed in only a few data points selected from a large set of data spreading over several different experiments. The number of data points selected is usually 100-200 and if divided into data sets containing points less than 120 s apart the total number of data sets usually is between 30 and 50. These data sets can be simulated independently which means that the parameter estimation can be performed in a parallelized manner as described in the previous section. The computers on any of Chalmers' clusters does not have more than 16 cores which means that more than one computer was needed to achieve maximum computational speed. The use of enough cores to simulate all data sets on different cores has some major drawbacks when considering computational efficiency:

1. The number of data sets will vary depending on how D-optimal design chooses the number of data points at different parameter values which means that there is no way to know beforehand how many cores will be needed. To ensure that the number of cores is high enough a number of cores will likely be unused for the entire simulation.
2. The residual and Jacobian calculation is performed on the total data set and can thereby not be parallelized over a large number of cores. These calculations are made frequently which means that the majority of the cores will be unused for a significant part of the parameter estimation.

Despite these drawbacks computational speed has usually been prioritized when performing parameter estimation and a large amount of cores have been allocated before these calculations have been performed.

6 RESULTS AND DISCUSSION

6.1 PAPER I – TRADITIONAL PARAMETER ESTIMATION ON A FULL SCALE DOC

Parameter tuning was performed against data from a full scale engine rig with standard set-up described in section 3.2. The experimental plan including catalyst configurations and engine operating points is described in section 3.2.2. The catalyst model where the catalyst washcoat was discretized as tanks in series both radially and axially is described in section 4.1 and the global kinetic model used is described in section 4.2. Four different modeling approaches were used for parameter tuning to demonstrate the advantages of radially discretizing the washcoat, including internal transport resistance in the catalyst model, and evaluate possible benefits from tuning mass transport parameters

6.1.1 MODES OF PARAMETER ESTIMATION

The four different modeling approaches (modes) for parameter estimations are summarized in table. 4.

TABLE 4 *Short description of the modes of Parameter Estimation*

Nr.	Modes of Parameter Estimation	Number of parameters	Discretization	
			Segments	Layers
1	Undiscretized washcoat and fixed effective diffusivity	17	10	2
2	Negligible internal mass transfer resistance	17	10	8*
3	Discretized washcoat and fixed effective diffusivity	17	10	8
4	Discretized washcoat and tuned effective diffusivity	19	10	8

*Since no concentration gradients in the washcoat were expected two layers would have been enough for this case, however eight layers were used for computational consistency

In Mode 1 the model was simplified to only contain two layers. The outer layer was selected to be only 2% of the total washcoat which meant that external mass transfer was the dominating resistance between the gas bulk and outer layer. This mode demonstrates a model that is computational less demanding where internal transport resistance is present although poorly resolved. Mode 2 also represents a case with discretization of the washcoat, however effective diffusivities were set to very high values (1000 times initial estimates). In effect, Mode 2 is a case with negligible internal transport resistance. Mode 3 and Mode 4 differ only by the fact that the latter has enabled estimation of the effective diffusivity whereas the former has not. For Mode 3 as with Mode 1 the effective diffusivities were fixed at the initially estimated values (see section 5.1.3).

6.1.2 HEAT TRANSFER PARAMETER TUNING

The heat transfer parameters thermal mass, environmental temperature, and lumped heat transfer coefficient were tuned before any additional parameter tuning was performed. Judging from the final parameter values there were a noticeable heat loss which also lead to radial temperature gradients in the monolith. These radial temperature gradients were also confirmed by measurement data where temperature was measured at 0%, 50%, 75%, and 100% of the total radius. The measurement data also showed that the temperature gradients between 0%, 50%, and 75% of the total radius generally were small but large between 75% and 100% of the total radius. A

reduced distance between the measurement points close to the total radius would have been needed to further evaluate the validity of the one channel model for the data at hand.

6.1.3 TUNING OF KINETIC- AND MASS TRANSFER PARAMETERS

A brief overview of the results is here presented highlighting the main conclusions from the parameter estimations performed. For a full presentation of the final parameter values and a detailed discussion thereof please see section 3.2 in the enclosed Paper I. The parameters in the kinetic expressions are shown in equations 2 to 7. The most important observations of the final kinetic- and mass transfer parameters can be summed up in the following points:

- A_6 and $E_{A,6}$ in common denominator G (see equation 6) had no significance for the simulation results.
- Under equal conditions the reaction rates of Mode 3 were significantly larger than the reaction rates of Mode 2 showing that the kinetic parameters in Mode 3 needed to compensate for a stronger transport resistance
- In Mode 4, which was the only mode where the effective diffusivity was tuned, the final effective diffusivity was increased by 7.71, and 2.11 times the original values for large components, and small components. These values are both still physically reasonable, see section 5.1.3 for a thorough description of the effective diffusivity.
- The differences between activation energies for the modes were relatively small and usually they were close to their initial values which could indicate that the activation energies are not as case specific as the pre-exponential factors.

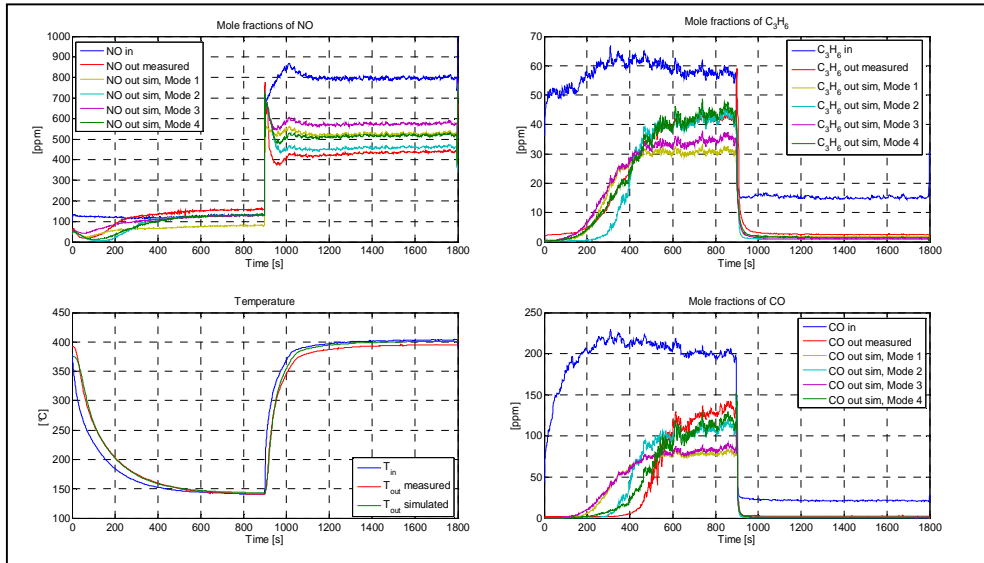


FIGURE 17 Measured and simulated outlet concentrations and temperature for a change in operating point from 2 to 8 for catalyst configuration with 0.59 wt%Pt and 0.11 mm washcoat thickness..

Figure 17 shows that only the model where transport resistance was neglected (Mode 2) shows a good fit for NO. Both Mode 1 and 3 had a poor fit for the CO transient and appear to approach the wrong stationary values for both HC and CO. The transient behaviour of both HC and CO, before the change in operating point, was caught well by Mode 4 but was a bit weaker for Mode 2. Both these modes approach the same stationary concentrations for HC (very good) and CO (good).

The above figure show only one of 16 transients used for parameter estimation (4 catalyst configurations and 4 operating point changes for every configuration). To give a broader overview of the simulation results the residual sum squares for every mode and component is shown in table 5. Note that the residuals in this table have been weighted with the inverse of the average outlet concentrations for the entire data set.

TABLE 5 Residual sum square ($\times 10^5$) of every component together with the summation of residual sum square (rightmost column) for the different modes.

	NO	HC	CO	NO ₂	Sum
Mode 1	4.77	4.26	12.4	5.80	27.3
Mode 2	0.67	3.10	4.46	0.83	9.05
Mode 3	2.09	2.44	6.89	2.64	14.1
Mode 4	0.77	2.41	3.49	0.97	7.65

Looking at the results of the different modes of parameter estimation with respect to both the residual sum squares (table 5) and figure 17 it is obvious that it was not possible to obtain a good fit with a washcoat that was not discretized radially at the default values of effective diffusivities (Mode 1).

The starting kinetic parameters shown in table 3 were collected from lab scale data, where the transport resistance was assumed to be negligible. It may be speculated that the difficulties encountered when tuning a model where the transport resistance is not neglected could indicate that the original parameters were in fact influenced by transport resistance, a phenomena observed previously [52]. The structure of the kinetic model itself may also make it less suitable for a catalyst model where the internal transport resistance is clearly separated from the kinetics. The foundation of this conclusion is that the sign of the activation energy (or heat of adsorption) for NO inhibition ($E_{A,7}$) is positive and thus will reduce reaction rates with increased temperature in a similar way that internal transport resistance would. This could then explain why the results of Mode 2, where the transport resistance was neglected, showed a better fit for NO_x which can be seen in both table 5 and the figure 17. In a model that clearly separates mass transport and kinetics, it is in other words not only important to have original parameters uninfluenced by transport resistance but also that the kinetic model itself is not constructed to mimic internal transport effects.

The overall fit of Mode 4 is significantly better than the overall fit of Mode 3 which is also evident when the total residual sum of squares are compared (table 5). This would indicate that the tuning of transport resistance parameters is very important for the overall behaviour of the model.

6.2 PAPER II – PARAMETER ESTIMATION WITH MVDA ON A FULL SCALE DOC

In this paper two different approaches to the method presented in section 5.3 were evaluated. The method was performed on the same data as in Paper I which means that experimental design and data collection will not be further discussed here.

6.2.1 MVDA APPROACHES

In the first approach the number of steps taken with the gradient search method in the points selected with MVDA was limited to only one. The motivation for this approach was that the points selected with MVDA were selected by evaluating the sensitivity for all data points (Jacobian matrix) for a defined set of parameter values. When the parameter values are changed, like they are during a gradient search, the sensitivity will also change and the point selection should be updated to ensure that the parameter estimation is performed in the statistically best data points. By limiting the number of steps to one, new points will be selected every time an improved set of parameter values is found. The drawback with the method is that the sensitivity for all data points needs to be frequently calculated. This is time consuming since all time points are used for these calculations and more time will be spent selecting new data points than for performing actual parameter estimation in the selected data points. This method will be referred to as “MVDA 1 step”.

In the second approach, referred to as “MVDA 5 step”, the number of steps taken with the gradient search method (in the points selected with MVDA) was instead limited to 5. Since the steps with the gradient search method will still be limited the parameter values will change little from the starting values and the selected time points should still be relevant. As a result more computational time will be spent on parameter estimation compared to the MVDA 1 step method.

6.2.2 FIT TO MEASUREMENT DATA COMPARISON

The fit of the temperature simulation was considered good enough in Paper I and as a result only tuning of the kinetic and mass transport parameters were performed with the MVDA method. Two examples of the final results of the parameter estimation with the two MVDA approaches are shown in figure 18. The two modes of parameter estimation that gave the best fit in Paper I (Mode 2 and 4 described in table 4) are also included in the figures as a reference.

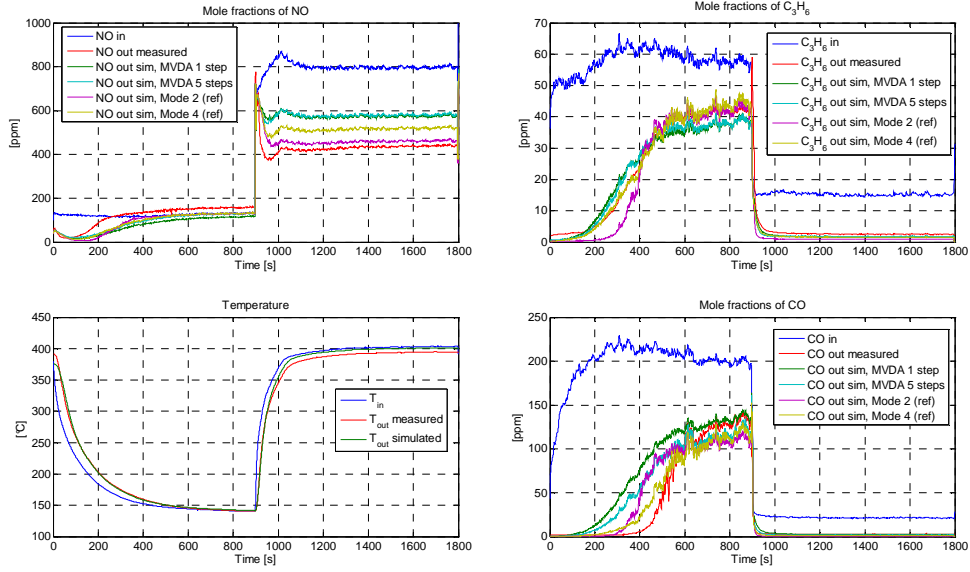


FIGURE 18 Measured and simulated outlet concentrations and temperature for a change in operating point from 2 to 8 for catalyst configuration with 0.59 wt% Pt and 0.11 mm washcoat thickness.

Figure 18 shows that both the parameters estimated with the MVDA 1 step approach and the parameters estimated with the MVDA 5 step approach had a poor fit for NO at high temperatures which is also noticeably worse than for the reference estimations. This is also true for CO, especially for the MVDA 1 step approach, even though the general fit is better than for NO.

The above graph show only one of 16 transients used for parameter estimation (4 catalyst configurations and 4 operating point changes for every configuration). To provide a broader overview of the simulation results the residual sum squares for every component is shown in table 6. Note that the residuals in this table have been weighted with the inverse of the average concentrations for the entire data set.

TABLE 6 Residual sum square ($\times 10^5$) of every component together with the summation of residual sum square (rightmost column) for the different modes.

	NO	HC	CO	NO ₂	Sum
MVDA 1 step	2.82	1.80	17.00	3.44	25.06
MVDA 5 step	1.71	1.83	12.52	2.13	18.19
Mode 2 (ref)	0.67	3.10	4.46	0.83	9.05
Mode 4 (ref)	0.77	2.41	3.49	0.97	7.65

If the results in table 6 and figure 18 are studied it is evident that the parameter estimation with the MVDA methods generates a noticeably inferior

fit for NO_x and CO and better fit for HC than the traditional parameter estimation methods shown as references. One reason for the poor fit of NO_x is probably the weighting of the residuals. NO and NO_2 outlet concentrations are high over the entire data set which means that the average concentration will be high and the weighting of the NO_x residuals will thereby be low. The low weight will be balanced by the high number of points where the outlet concentrations are non zero in the full data set. The average outlet concentrations of HC and CO are low since the engine out concentrations of HC and CO are close to zero at most engine operating points. The weights of HC and CO residuals will therefore be high and the few points where the outlet concentrations are non zero will have a large influence on the total residual sum of squares. If parameter estimation is performed on all points the residual weighting will be fair and assure that no component has a dominating influence.

With the MVDA data point selection a few points that have high sensitivity for the different parameters and residuals will be chosen. Since HC, CO, NO and NO_2 residuals are weighted to have equal contributions to the residuals of the full data set, same influence on the Jacobian matrix, about the same number of points that have high influence of the different component residuals will be chosen. This means that about a fourth of the points will be chosen since the influence on the HC residual is high which will occur where the outlet concentration of HC is non zero. The relative number of points where HC and CO are high will thereby be much larger in the points selected by MVDA than for the full data series. The parameter estimation will prioritize the minimization of HC and CO residuals since they will have the largest influence on the total residual sum of squares.

6.2.3 COMPUTATIONAL EFFICIENCY COMPARISON

In addition to an improved fit of the final result the objective of the parameter estimation method with MVDA was to reduce computational demand. A summary of the computational times for the reference cases from Paper I and from the two approaches in Paper II are shown in table 7.

TABLE 7 *Computational time for the parameter estimations performed in Paper II compared with the reference cases from Paper I*

	Total simula- tion time [h]	Number of cores used	Core hours used	Iterations
MVDA 1 step	479	48	22992	8*
MVDA 5 step	686	48	32928	10*
Mode 1 (ref)	61	16	976	17
Mode 2 (ref)	230	16	3680	13
Mode 3 (ref)	635	16	10160	37
Mode 4 (ref)	422	16	6752	21

* Number of times a improved parameter value have been found through parameter estimation in the data points selected with MVDA (right hand loop performed in figure 14)

The reference estimations were run until the reduction in the residual sum of squares was below 1% for three consecutive steps with the gradient search method. The MVDA approaches had the same criteria applied for the residual sum of squares for the total data set. As an additional criterion the estimation would be halted if no improved parameter values were found after more than ten selections of data points for the same parameter values (corresponding to more than ten left hand loops in figure 14).

The total computational time varies considerably between the different cases. The simple model with the low discretization (Mode 1) has the shortest computational time since the iteration time is significantly shorter than for the other cases. For the other reference cases the number of iterations is the determining factor but it is hard to draw any conclusion about why one model converges faster than the others. The use of the computational resources with the MVDA method is less efficient than the traditional reference methods which can be seen if the numbers of core hours are compared for the different cases (for further discussion see section 5.4.2).

When the system of differential equations that describes the catalyst model is solved the computational time will be very dependent on the behavior of the time dependence of the inlet conditions. The faster the inlet conditions change the more the dependent variables in the catalyst will change which result in increased calculation times. Even though the number of points selected with MVDA is low the majority of them will be selected where the inlet data is very transient. This means that the parts of the total data series that are most time consuming to simulate will also be included in the simulation with the reduced

number of points. Even though the number of data points selected with MVDA is less than 1% of the total data series the simulation time will still be about 25% of the simulation time of the total data series.

The high parameter sensitivity in transient data points indicated by the preference from MVDA could mean that a better fit could be achieved if more transient data was available. This issue will be addressed in Paper III.

6.2.4 CONCLUSIONS

The method of parameter tuning presented in the current study did not obtain a better overall fit to measurement data than a parameter tuning performed with a standard method used as reference. Neither was the simulation time reduced. Some areas of possible improvement of the method were identified:

- The residuals should not be scaled against the inverse of the average concentration over the total data set. The influence of components with low average concentration but high peak values will dominate the parameter estimation with the investigated method.
- The high parameter sensitivity in transient data points indicated by the preference from D-optimal design could mean that a better fit could be achieved if more transient data was available.
- The parameter sensitivity will develop as the parameters are tuned. The parameter scaling could therefore be updated continuously to avoid that the parameter tuning method is dominated by a few parameters with a large influence on the residuals.

Of the two parameter estimation methods evaluated the method where five steps in parameter space were taken before new data points were selected with MVDA gave the best fit to measurement data.

6.3 PAPER III – NEW METHODOLOGY FOR TRANSIENT ENGINE RIG EXPERIMENTS

In this section two examples of results from experimental types 2 and 3 described in section 3.3.2 will be shown as a demonstration of the exhaust gas compositions made possible by the Scania engine rig set-up.

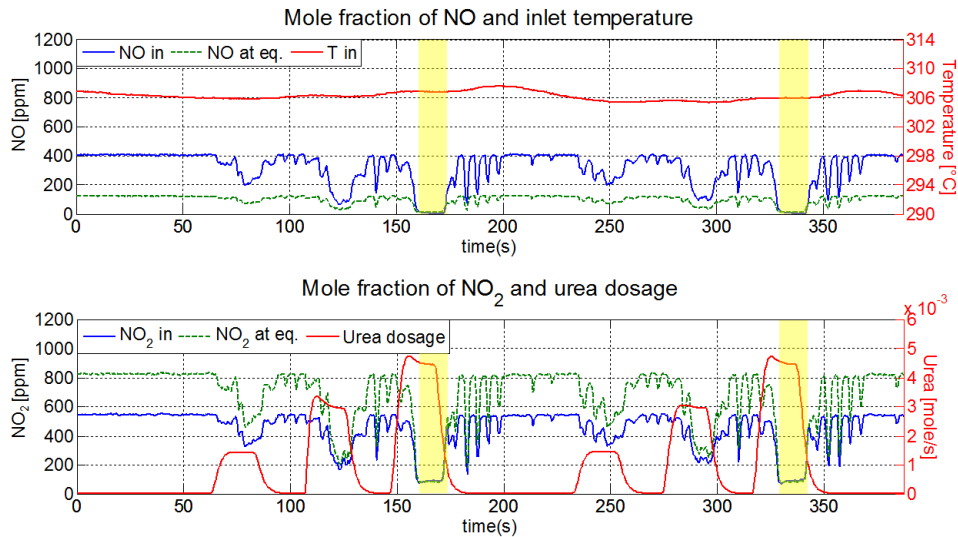


FIGURE 19 NO and NO_2 concentrations, and temperature in the test object inlet, and urea dosage for one experiment of type 2.

In figure 19 one experiment of type 2 is shown. In this type of experiment the SCR and urea injection makes it possible to achieve a wide range of NO_2/NO_x ratios and concentrations. Two cycles with increasing urea dosage (0%, 30%, 60% and 90% of stoichiometric NO_x reduction) were performed in the experiment. For the results shown in figure 19 valve 2 was closed and valve 1 was fully open (see figure 8 for engine rig layout). A NO_x composition containing close to 100% NO_2 can be observed at high urea dosages for some cases (see yellow marking in graphs). CO and HC concentrations are not shown since the conversions of these components were close to 100%.

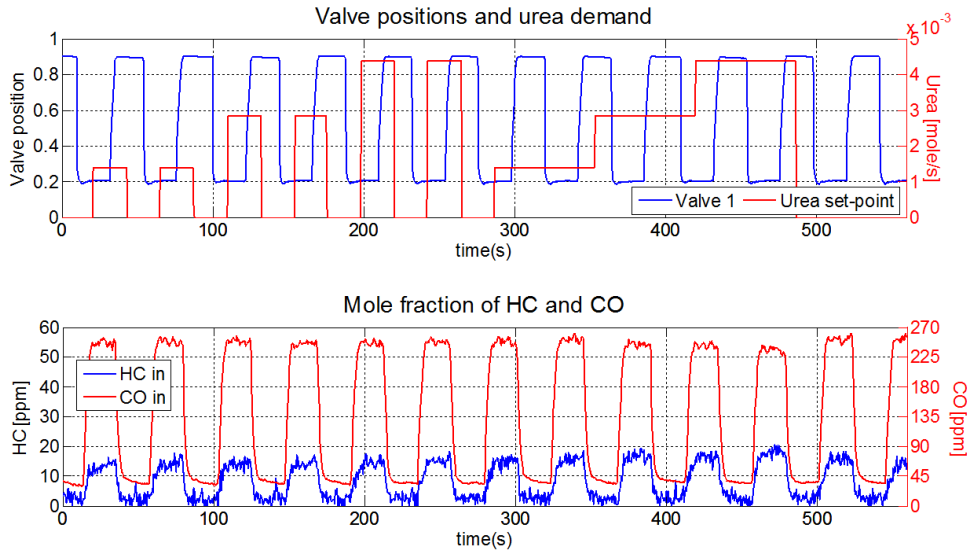


FIGURE 20 HC and CO concentrations, valve 1 position, and set-point for urea dosage for one experiment of type 3

Figure 20 and figure 21 show the results of one experiment of type 3. Figure 20 shows sequences where the CO concentration is high at the same time as the HC concentration is close to zero; this behavior is even more pronounced for experiments performed at engine operating points with higher exhaust temperatures. Figure 20 also shows that both HC and CO are unaffected by the urea injection.

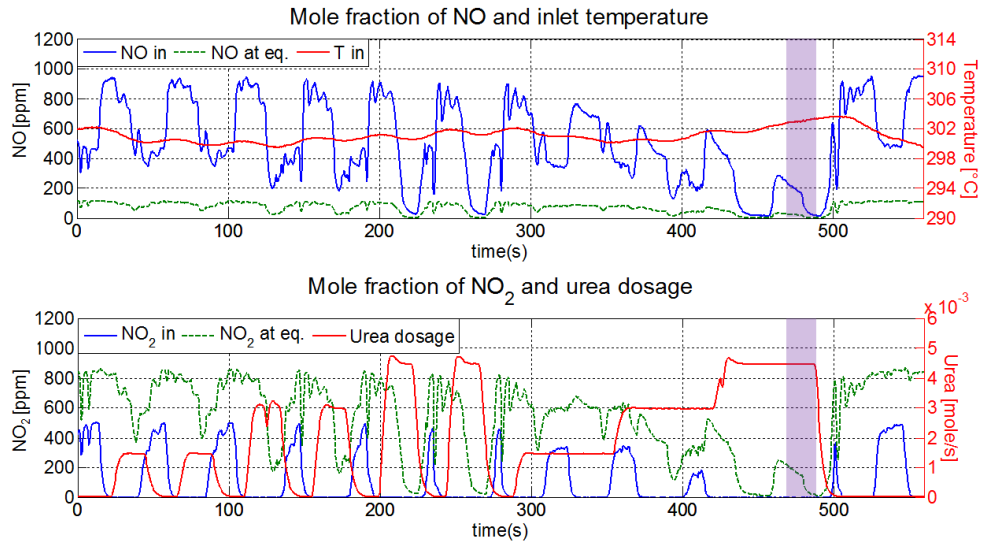


FIGURE 21 *NO* and *NO*₂ concentrations, temperature, and urea dosage for one experiment of type 3.

Figure 21 shows that *NO* and *NO*₂ are affected by both the urea injection and the *DOC* bypass ratio. At high urea injection all *NO*₂ and most *NO* are consumed. Purple markings show time points where *CO* concentration exceeds *NO*_x concentration

The most apparent advantage with the experimental set-up is the possibility to achieve fast transients in concentration with only small variations in temperature. The experimental data has, however, also shown that the following engine rig exhaust gas features are enabled by the experimental set-up that would not be possible with a standard engine rig:

- High *CO* concentrations with *HC* concentrations close to zero
- *HC* concentrations exceeding *NO*_x concentration
- *NO* concentrations close to zero with significant *NO*₂ concentration

The reduced correlation between temperature and concentrations, but also between individual concentrations, significantly widen the possible experimental conditions available and may be of great aid in full scale parameter tuning and catalyst modeling.

7 CONCLUSIONS

Several conclusions could be drawn from the parameter estimation performed in Paper I both regarding the kinetic model and the catalyst model. The conclusions that will be of most importance for the future work in the project are presented here.

The most important conclusion from Paper I was that the best fit with a catalyst model with internal transport resistance could be achieved if some parameters affecting the internal mass transport (in this study effective diffusivity) were tuned in addition to the kinetic parameters. This indicated that internal transport limitations can be of importance for a DOC in a heavy-duty vehicle aftertreatment system, particularly for HC oxidation but also to a certain extent for NO and CO oxidation. This was also confirmed when the simulated reaction rates and diffusion rates were compared by calculation of the Weisz modulus.

The simultaneous tuning of kinetic parameters and mass transport parameters depend on an experimental design for this purpose. In the study it was shown that the experimental plan should span both transient and stationary experimental data as well as a wide range of different catalyst configurations. By tuning parameters to data from engine measurements on different catalysts with different kinetic and mass transport properties the correlation between the kinetic and transport parameters was reduced.

The study also showed that it is still possible to obtain a good fit for a model with negligible internal transport resistance since kinetic parameters could compensate for transport limitations. This highlighted the inherent difficulties

using kinetic models with high parameter correlation and also showed the importance of using a kinetic model that has an intrinsic kinetic structure.

The parameter estimation performed with the MVDA methods presented in Paper II did not result in a better fit than the traditional method presented in Paper I, neither was the computational demand less. Some important conclusions were however made that will lead to future studies of how the method can be improved.

During the analysis of the results it became apparent that the scaling of the residuals is of great importance for the parameter tuning in points selected with MVDA. To get a good fit it is not appropriate to scale against average outlet concentration in the whole data series since this will greatly benefit components of low average concentrations.

Another conclusion is that the simulation time is not reduced compared to the standard method of parameter estimation. One reason is that the points selected with MVDA mainly are in transient regions that are computationally costly to simulate. Another reason could be that the aforementioned scaling which, if improved, would lead to faster convergence and a shorter simulation time.

8 OUTLOOK

Overall the fit of the results from the evaluated methods in Paper I and Paper II could be improved. The results from methods aided by MVDA in Paper II is not that far off from the results from the more standard method of parameter tuning presented in Paper I. This indicates that it is not only the method with MVDA that needs to be improved but maybe also the experimental design and formulation of the catalyst model.

As described in the previous chapter the kinetic model used [11] may be of a structure that has parameters able to account for transport resistance. This is highly undesirable in a model that strives to separate kinetics and mass transport. Other possible weaknesses with the kinetic model used so far include the fact that it does not account for accumulation of adsorbed surface species and it excludes other possibly important reactions, like NO₂ oxidation of HC and CO. A suitable compromise may be a kinetic model including only the most abundant adsorbed species, i.e. more like a microkinetic model but still relatively computationally expedient. A different kinetic model will therefore be used for the modeling of the data generated in the experiments described in Paper III. These experiments will hopefully also benefit the MVDA method of parameter tuning since a much wider span of transient data will be available (more than 200 different transients will be available which is to be compared with 16 transients in the data used in Paper I and Paper II).

An issue that has been mentioned but not thoroughly discussed is the radial temperature gradients in the monolith. These gradients exist and have been measured in the data used in Paper I and II and will make the one channel model less applicable. In the experimental set up in Paper III the piping

upstream of the DOC has therefore been insulated to reduce the temperature gradients in the flow entering the DOC and thereby reducing the temperature gradients in the catalyst.

Both the standard method of parameter estimation presented in Paper I and the MVDA method presented in Paper II will be applied to the data from the experiments performed on the Scania engine rig (Paper III). The methods will however be updated from the experience gained in the project thus far which means that only Mode 4 from Paper I will be applied and that the residual scaling for the MVDA method will be improved.

BIBLIOGRAPHY

1. Heck, R.M. and R.J. Farrauto, *Automobile exhaust catalysts*. Applied Catalysis A: General, 2001. **221**(1–2): p. 443-457.
2. Stone, R., *Introduction to internal combustion engines / Richard Stone*. 1992, Houndmills, Basingstoke [England] :: Macmillan.
3. Thom, S.R., *Hyperbaric-Oxygen Therapy for Acute Carbon Monoxide Poisoning*. New England Journal of Medicine, 2002. **347**(14): p. 1105-1106.
4. Kao, L. and K. Nanagas, *Toxicity associated with carbon monoxide*. Clinics in Laboratory Medicine, 2006. **26**: p. 28.
5. Pârvolescu, V.I., P. Grange, and B. Delmon, *Catalytic removal of NO*. Catalysis Today, 1998. **46**(4): p. 233-316.
6. (ARB), C.A.R.B., *Findings of the Scientific Review Panel On The Report on Diesel Exhaust*. 1998.
7. de Kok, T.M.C.M., et al., *Toxicological assessment of ambient and traffic-related particulate matter: A review of recent studies*. Mutation Research/Reviews in Mutation Research, 2006. **613**(2–3): p. 103-122.
8. Auvray, X., *Vehicle emission abatement: NO oxidation and ammonia SCR*. 2011, Chalmers University of Technology.
9. van Setten, B., M. Makkee, and J. Moulijn, *Science and technology of catalytic diesel particulate filters*. CATALYSIS REVIEWS-SCIENCE AND ENGINEERING, 2001. **43**: p. 76.
10. Nova, I., et al., *NH₃–NO/NO₂ chemistry over V-based catalysts and its role in the mechanism of the Fast SCR reaction*. Catalysis Today, 2006. **114**(1): p. 3-12.
11. Voltz, S.E., et al., *Kinetic Study of Carbon Monoxide and Propylene Oxidation on Platinum Catalysts*. Product R&D, 1973. **12**(4): p. 294-301.
12. Lundstedt, T., et al., *Experimental design and optimization*. Chemometrics and Intelligent Laboratory Systems, 1998. **42**(1–2): p. 3-40.
13. Montgomery, D.C., *Design and Analysis of Experiments (7th Edition)*, John Wiley & Sons. p. 417-439.
14. Berger, R.J., et al., *Dynamic methods for catalytic kinetics*. Applied Catalysis A: General, 2008. **342**(1–2): p. 3-28.
15. Buzzi-Ferraris, G. and F. Manenti, *Kinetic models analysis*. Chemical Engineering Science, 2009. **64**(5): p. 1061-1074.
16. Martens, H. and T. Naes, *Multivariate Calibration*. 1989: John Wiley & Sons.
17. Dieselnets. *Swedish Diesel Fuel Specifications*. 2013 [cited 2013 0215]; Available from: <http://www.dieselnets.com/standards/se/fuel.php>.
18. Kolaczkowski, S., et al., *Transient experiments on a full-scale DOC—Methodology and techniques to support modelling*. Catalysis Today, (0).
19. Sjoblom, J., *Bridging the gap between lab scale and full scale catalysis experimentation, in Capoc 2012*. Accepted for publication in Catalysis Today, 2012.
20. Kumar, A. and S. Mazumder, *Toward simulation of full-scale monolithic catalytic converters with complex heterogeneous chemistry*. Computers & Chemical Engineering, 2010. **34**(2): p. 135-145.
21. Štěpánek, J., et al., *Catalyst simulations based on coupling of 3D CFD tool with effective 1D channel models*. Catalysis Today, 2012. **188**(1): p. 87-93.

22. Stamatelos, A.M., et al., *Computer aided engineering in diesel exhaust aftertreatment systems design*. Proceedings of the Institution of Mechanical Engineers, Part D (Journal of Automobile Engineering), 1999. **213**(Copyright 2000, IEE): p. 545-60.
23. Güthenke, A., et al., *Current status of modeling lean exhaust gas aftertreatment catalysts*, in *Advances in Chemical Engineering*, B.M. Guy, Editor. 2007, Academic Press. p. 103-283.
24. Metkar, P.S., M.P. Harold, and V. Balakotaiah, *Experimental and kinetic modeling study of NH₃-SCR of NO_x on Fe-ZSM-5, Cu-chabazite and combined Fe- and Cu-zeolite monolithic catalysts*. Chemical Engineering Science, 2013. **87**(0): p. 51-66.
25. Ericson C, W.B., Odenbrand I, *A state-space simplified SCR catalyst model for real time applications*. SAE SP, NUMB 2155, 2008: p. 7.
26. Mladenov, N., et al., *Modeling of transport and chemistry in channel flows of automotive catalytic converters*. Chemical Engineering Science. **65**(2): p. 812-826.
27. Tronconi, E. and P. Forzatti, *Adequacy of Lumped Parameter Models for SCR Reactors with Monolith Structure*. Aiche Journal, 1992. **38**(2): p. 201-210.
28. Fogler, H.S., *Elements of chemical reaction engineering*. Prentice Hall international series in the physical and chemical engineering sciences, ed. ed. 2006, Upper Saddle River, N.J.: Prentice Hall/PTR.
29. Lafossas, F., et al., *Calibration and Validation of a Diesel Oxidation Catalyst Model: from Synthetic Gas Testing to Driving Cycle Applications*. 2011.
30. Ansell, G.P., et al., *The development of a model capable of predicting diesel lean NO_x catalyst performance under transient conditions*. Applied Catalysis B: Environmental, 1996. **10**(1-3): p. 183-201.
31. Watling, T.C., et al., *Development and Validation of a Pt-Pd Diesel Oxidation Catalyst Model*. Number: 2012-01-1286, 2012.
32. Crocoll, M., S. Kureti, and W. Weisweiler, *Mean field modeling of NO oxidation over Pt/Al₂O₃ catalyst under oxygen-rich conditions*. Journal of Catalysis, 2005. **229**(2): p. 480-489.
33. Olsson, L., et al., *Mean field modelling of NO_x storage on Pt/BaO/Al₂O₃*. Catalysis Today, 2002. **73**(3-4): p. 263-270.
34. Salomons, S., et al., *CO and H₂ oxidation on a platinum monolith diesel oxidation catalyst*. Catalysis Today, 2006. **117**(4): p. 491-497.
35. Chorkendorff, I. and J.W. Niemantsverdriet, *Concepts of modern catalysis and kinetics*. 2003: Wiley-VCH.
36. Oh, S.H. and J.C. Cavendish, *Transients of monolithic catalytic converters. Response to step changes in feedstream temperature as related to controlling automobile emissions*. Industrial & Engineering Chemistry Product Research and Development, 1982. **21**(1): p. 29-37.
37. Wang, T.J., S.W. Baek, and J.H. Lee, *Kinetic parameter estimation of a diesel oxidation catalyst under actual vehicle operating conditions*. Industrial & Engineering Chemistry Research, 2008. **47**(8): p. 2528-2537.
38. Pandya, A., et al., *Global kinetic model and parameter optimization for a diesel oxidation catalyst*. Topics in Catalysis, 2009. **52**(13-20): p. 1929-1933.
39. Kandylas, I.P. and G.C. Koltsakis, *NO₂-Assisted Regeneration of Diesel Particulate Filters: A Modeling Study*. Industrial & Engineering Chemistry Research, 2002. **41**(9): p. 2115-2123.

40. Guojiang, W. and T. Song, *CFD simulation of the effect of upstream flow distribution on the light-off performance of a catalytic converter*. Energy Conversion and Management, 2005. **46**(13–14): p. 2010-2031.
41. Tsinoglou, D.N. and G.C. Koltsakis, *Effect of perturbations in the exhaust gas composition on three-way catalyst light off*. Chemical Engineering Science, 2003. **58**(1): p. 179-192.
42. Koltsakis, G.C. and A.M. Stamatelos, *Modeling dynamic phenomena in 3-way catalytic converters*. Chemical Engineering Science, 1999. **54**(20): p. 4567-4578.
43. Dubien, C., et al., *Three-way catalytic converter modelling: fast- and slow-oxidizing hydrocarbons, inhibiting species, and steam-reforming reaction*. Chemical Engineering Science, 1998. **53**(3): p. 471-481.
44. Koltsakis, G.C., P.A. Konstantinidis, and A.M. Stamatelos, *Development and application range of mathematical models for 3-way catalytic converters*. Applied Catalysis B: Environmental, 1997. **12**(2–3): p. 161-191.
45. Chen, D.K.S., et al., *A Three-Dimensional Model for the Analysis of Transient Thermal and Conversion Characteristics of Monolithic Catalytic Converters*. 1988, SAE International, Paper number. 880282.
46. Tronconi, E. and A. Beretta, *The role of inter- and intra-phase mass transfer in the SCR-DeNO(x) reaction over catalysts of different shapes*. Catalysis Today, 1999. **52**(2-3): p. 249-258.
47. Sjoblom, J. and D. Creaser, *Latent variable projections of sensitivity data for experimental screening and kinetic modeling*. Computers & Chemical Engineering, 2008. **32**(12): p. 3121-3129.
48. Box, G.E.P., et al., *Some Problems Associated with the Analysis of Multiresponse Data*. Technometrics, 1973. **15**(1): p. 33-51.
49. Hauff, K., et al., *A global description of DOC kinetics for catalysts with different platinum loadings and aging status*. Applied Catalysis B: Environmental, 2010. **100**(1–2): p. 10-18.
50. Froment, G.F., J. De Wilde, and K.B. Bischoff, *Chemical reactor analysis and design*. Vol. 3rd ed. 2011, Hoboken, N.J: Wiley.
51. Coleman, T.F. and Y.Y. Li, *An interior trust region approach for nonlinear minimization subject to bounds*. Siam Journal on Optimization, 1996. **6**(2): p. 418-445.
52. Wickman, B., et al., *Modeling mass transport with microkinetics in monolithic NO x storage and reduction catalyst*. Topics in Catalysis, 2007. **42-43**(1-4): p. 123-127.

